Further Studies of Cluster-Bound Imido Ligands. Imido–Acyl Coupling and Promotion of the Formation and Carbonylation of Imido Ligands by Halides

Sung-Hwan Han, Jeong-Sup Song, Phillip D. Macklin, Sonbinh T. Nguyen, and Gregory L. Geoffroy*

Department of Chemistry, The Pennsylvania State University, University Park, Pennsylvania 16802

Arnold L. Rheingold

Department of Chemistry, University of Delaware, Newark, Delaware 19716

Received January 9, 1989

Halides, cyanide, and hydride ligands have been shown to promote the formation of imido ligands from nitrosobenzene as evidenced by the rapid reaction which occurs to form the cluster anions $[Ru_3(\mu_3\text{-NPh})(X)(CO)_9]^-$ (X = Cl, Br, I, CN, H) when nitrosobenzene is added to solutions of $[Ru_3(X)(CO)_n]^-$ (n = 10, 11). The halide and cyanide derivatives also result from addition of the appropriate $[(Ph_3P)_2N]X$ salt to the imido cluster $Ru_3(\mu_3\text{-NPh})(CO)_{10}$. The salt $[Na(18\text{-crown-6})][Ru_3(\mu_3\text{-NPh})(I)(CO)_9]$ has been structurally characterized: $P\bar{1}$, a = 10.369 (3), b = 13.335 (3), c = 13.738 (3) Å, α = 79.54 (2), β = 77.03 (2), γ = 86.76 (2)°, V = 1820.1 (6) Å^3, Z = 2, $R(F)$ = 4.55%, $R(wF)$ = 5.20% for 5663 reflections ($4\sigma(F_o)$). Its structure is similar to that of the parent cluster $Ru_3(\mu_3\text{-NPh})(CO)_9(\mu_3\text{-CO})$, with the iodide having replaced a CO in a position trans to the μ_3-CO ligand. The anion promotion of the nitrosobenzene deoxygenation reaction is believed to result from the anions promoting loss of CO and formation of an intermediate with a coordinated nitrosobenzene which quickly deoxygenates to form CO_2 and the imido ligand. Support for this suggestion comes from the observation that the cluster $Ru_3(\mu_3\text{-NPh})(CO)_{10}$ rapidly forms in high yield upon addition of PhNO to $Ru_3(CO)_{11}(CH_3CN)$. Similar reactions of PhNO and Bu^{t}NO with acetonitrile-substituted clusters have been used to prepare $Os_3(\mu_3\text{-NPh})(CO)_{10}$, the new heteronuclear clusters $Fe_2Ru(\mu_3\text{-NPh})(CO)_{10}$ and $FeRu_2(\mu_3\text{-NPh})(CO)_{10}$, and the mixed-substituent bis(imido) cluster $Ru_3(\mu_3\text{-NPh})(\mu_3\text{-NBu}^t)(CO)_9$. The heteronuclear cluster anion $[CoRu_2(\mu_3\text{-NPh})(CO)_9]^-$ has also been prepared by a metal-exchange reaction via addition of $[Co(CO)_4]^-$ to $Ru_3(\mu_3\text{-NPh})(CO)_{10}$. Protonation of this anion gives the hydride cluster $HCoRu_2(\mu_3\text{-NPh})(CO)_9$ which has been structurally characterized: $P\bar{1}$, a = 8.609 (2), b = 15.547 (4), c = 15.721 (4) Å, α = 85.07 (2), β = 75.97 (2), γ = 79.58 (2)°, V = 2005.8 (9) Å^3, Z = 4, $R(F)$ = 4.17%, $R(wF)$ = 5.26% for 5172 reflections ($3\sigma(F_o)$). The cluster consists of a $CoRu_2$ triangle with a triply bridging imido ligand and with the hydride bridging the two Ru atoms. Halides have also been found to promote the carbonylation of imido ligands to form isocyanates as illustrated by the rapid reactions which occur to form PhN=C=O when the cluster anions $[Ru_3(\mu_3\text{-NPh})(X)(CO)_9]^-$ (X = Cl, Br, I) are placed under 1 atm of CO at 22 °C. In contrast, the cluster anions $[Ru_3(\mu_3\text{-NPh})(X)(CO)_9]^-$ (X = CN, H) do not react with CO under these mild conditions, although the anion $[CoRu_2(\mu_3\text{-NPh})(CO)_9]^-$ readily carbonylates to form $Ru_3(CO)_{12}$, $[Co(CO)_4]^-$, and $[PhNCO]_2$ under slightly more forcing conditions. Acyl-substituted clusters $[Ru_3(\mu_3\text{-NPh})(CO)_9(C\{O\}R)]^-$ (R = Me, Ph) form upon reacting $Ru_3(\mu_3\text{-NPh})(CO)_{10}$ with the appropriate RLi reagent, and the acyl ligands in these clusters migrate to the imido ligands when placed under CO. The resultant amido clusters have been protonated to form the hydride species $HRu_3\{\mu_2\text{-N(Ph)C(O)R}\}(CO)_{10}$ which undergo reductive elimination of the amide PhNHC{O}R when placed under a CO atmosphere. The possible relevance of these various imido transformations to nitroaromatic carbonylation catalysis is discussed.

Introduction

A variety of nitrogen-containing products can be formed via reductive carbonylation of nitroaromatics,[1] and this route is particularly attractive for isocyanates and carbamates since it avoids the use of phosgene to prepare these important industrial chemicals.[2] Among the catalysts reported for nitroaromatic carbonylation is the one recently described by Cenini et al.[3] who showed that $Ru_3(CO)_{12}$ catalyzes the carbonylation of nitrobenzene in the presence of methanol to produce methyl *N*-phenylcarbamate and aniline and that the reaction is markedly dependent on the presence of halide promoters (eq 1). The conversion

$$PhNO_2 + MeOH + CO \xrightarrow[165°C,\ 82\ atm,\ 5\ h]{Ru_3(CO)_{12}} PhNH\text{-}C(=O)\text{-}OMe + Ph\text{-}NH_2 \quad (1)$$

toluene

promoter	conversion	carbamate yield	aniline yield
none	36%	22%	34%
$[Et_4N]^+Cl^-$	100%	93%	7%
$[Et_4N]^+I^-$	46%	64%	28%

(1) (a) Alessio, E.; Mestoni, G. *J. Organomet. Chem.* **1985**, *291*, 117. (b) Dieck, H. A.; Laine, R. M.; Heck, R. F. *J. Org. Chem.* **1975**, *40*, 2819. (c) Yamashita, M.; Mizushima, K.; Watanabe, Y.; Mitsudo, T.; Takegami, Y. *J. Chem. Soc., Chem. Commun.* **1976**, 670. (d) Nefedov, B. K.; Manov-Yuvenskii, V. I. *Izk, Akad. Nauk SSSR, Ser. Khim.* **1977**, *11*, 2597. (e) Nefedof, B. K.; Manov-Yuvenskii, V. I.; Khoshdurdyey, Kh. O.; Novikov, S. S. *Dokl. Akad. Nauk SSSR* **1977**, *232*, 1088. (f) Nefedov, B. K.; Manov-Yuvenskii, V. I.; Novikov, S. S. *Dokl. Akad. Nauk SSSR* **1977**, *234*, 1343. (g) Elleuch, B.; Taarit, Y. B.; Basset, J. M.; Kervennal, J. *Angew. Chem., Int. Ed. Engl.* **1982**, *21*, 687. (h) Weigert, F. J. *J. Org. Chem.* **1973**, *38*, 1316. (i) Hardy, W. B.; Bennet, R. P. *Tetrahedron Lett.* **1967**, 961. (j) Unverferth, K.; Hontsch, R.; Schwetlick, K. *J. Prakt. Chem.* **1979**, *321*, 928. (k) Braunstein, P.; Bender, R.; Kervennal, J. *Organometallics* **1982**, *1*, 1236 and references therein. (l) Braunstein, P.; Kervennal, J.; Richert, J.-L. *Angew. Chem., Int. Ed. Engl.* **1985**, *24*, 768. (m) Iqbal, A. F. M. *J. Org. Chem.* **1972**, *37*, 2791. (n) Watanabe, Y.; Tsuji, Y.; Kondo, T.; Takeuchi, R. *J. Org. Chem.* **1984**, *49*, 4451.

(2) (a) Arnold, R. G.; Nelson, J. A.; Verbanc, J. J. *Chem. Rev.* **1957**, *57*, 47. (b) Wilson, C. V. *Org. Chem. Bull.* **1963**, *35*, 2.

(3) (a) Cenini, S.; Cortti, C.; Pizzotti, M.; Porta, F. *J. Org. Chem.* **1988**, *53*, 1243. (b) Cenini, S.; Pizzotti, M.; Crotti, C.; Porta, F.; Monica, G. L. *J. Chem. Soc., Chem. Commun.* **1984**, 1286.

0276-7333/89/2308-2127$01.50/0

Scheme I

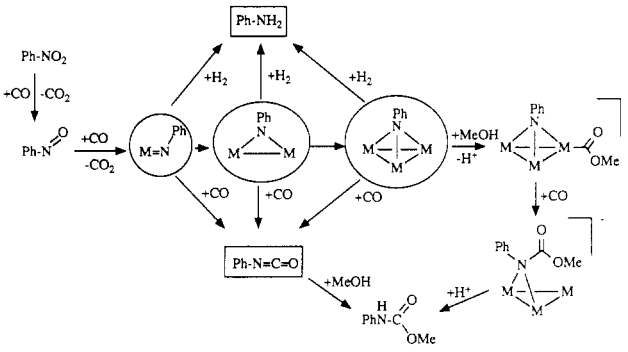

and selectivity to the desired carbamate was low in the absence of halide, but excellent selectivities and conversions were obtained when halides were present, with chloride being the superior promoter. Although a speculative rationalization of the halide-promoting effect was presented,[3] it has not been shown exactly why halides influence this catalytic reaction as they do. However, it is critically important to fully understand the basis for their action if the catalytic system is to be optimized.

The mechanism by which nitrobenzene is catalytically reduced to aniline and carbonylated to form carbamates has never been fully elucidated, although transformations like those shown in Scheme I have often been suggested.[4] This scheme implies the stepwise deoxygenation of nitrobenzene to form nitrosobenzene followed by subsequent nitrosobenzene deoxygenation to form an imido ligand bound to one, two, or three metal atoms. Hydrogenation of the imido ligand would yield aniline whereas carbonylation would give phenyl isocyanate. Reaction of the latter with alcohol would give the carbamate product. As also shown in Scheme I, carbamates could form via the coupling of imido ligands with alkoxycarbonyl ligands that are produced by alkoxide addition to a metal carbonyl.[4c] *However, it should be noted that there is no firm evidence that imido ligands and clusters are at all important in the catalytic chemistry*, and other mechanisms have been suggested involving initial reduction of nitrobenzene to aniline via an electron-transfer path[5] and the formation of carbamates via carbamoyl intermediates that are produced by addition of aniline to a carbonyl ligand.[6]

The goal of the present study was to test the validity of the mechanistic steps outlined in Scheme I through studies of appropriately chosen model compounds and particularly to explore the effect of halides on these transformations. Herein we show that halides dramatically promote both the formation of imido ligands from nitroso reagents and also the carbonylation of imido ligands to form isocyanates.[7] The coupling of imido and acyl ligands to form amido ligands has also been demonstrated, and several new mixed-metal imido clusters have been synthesized.

Results

Examination of the Effect of Halides on the $PhNO_2$ to PhNO Conversion. it is well-known from the early work of Sappa and Milone[8] that nitrobenzene reacts at elevated temperature with $Ru_3(CO)_{12}$ to form the imido clusters $Ru_3(\mu_3\text{-NPh})(CO)_{10}$ (**1**), and $Ru_3(\mu_3\text{-NPh})_2(CO)_9$ (**2**), (eq 2). Although the yields of the imido products were

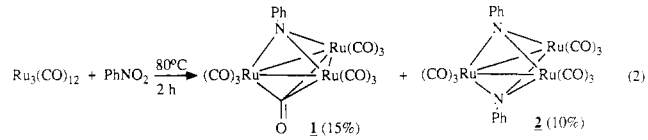

(2)

low, this reaction clearly demonstrates that $Ru_3(CO)_{12}$ can induce the deoxygenation of nitrobenzene to form imido ligands. To determine if halides would promote this reaction and permit it to proceed at lower temperatures, THF solutions of $PhNO_2$, $Ru_3(CO)_{12}$, and [PPN]X salts (PPN = $(Ph_3P)_2N$; X = Cl, Br, I) were stirred at 22 °C for 1 day. These reactions gave no conversion of $PhNO_2$ and only formation of the known cluster anions $[Ru_3(\mu_2\text{-X})(CO)_{10}]^-$ (X = Cl, Br, I), $[Ru_4(\mu_2\text{-X})(CO)_{13}]^-$, and $[Ru_3(\mu_3\text{-I})(CO)_9]^-$.[9] Under reflux conditions, reaction proceeded on the same time scale as that observed by Sappa and Milone,[8] but IR analysis indicated the formation of a complex mixture of products. It can be concluded that under these conditions halides do not significantly promote the deoxygenation of nitrobenzene.

Halide-Promoted Formation of Imido Ligands from Nitrosobenzene. Gladfelter and co-workers have shown that nitrosobenzene is a useful precursor for imido ligands, as illustrated by the preparation of cluster **1** shown in eq 3.[10] To explore the effect of halides and pseudohalides on this deoxygenation reaction, the reactions shown in eq 4 were examined. Clusters **3a–d**, which are known to

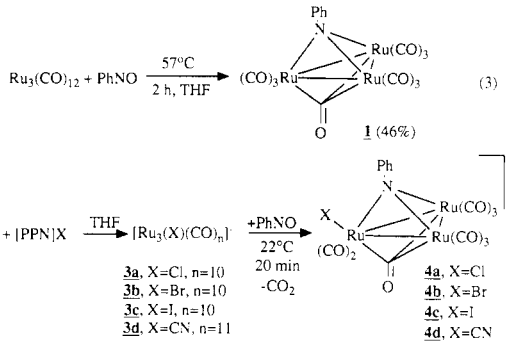

(3)

(4)

rapidly form when halides and $Ru_3(CO)_{12}$ are mixed,[9] were generated in situ, and nitrosobenzene was then added. In each case, rapid and quantitative reaction occurred to form the imido clusters **4a–d**. These latter species were also independently prepared by the direct reaction of **1** with halides (eq 5) and were characterized by their IR spectra

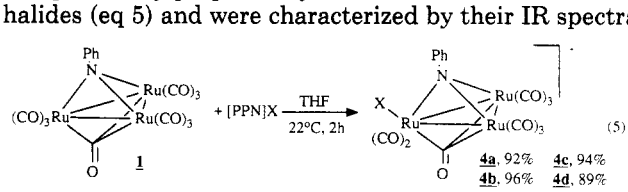

(5)

(4) (a) Cenini, S.; Pizzotti, M.; Crotti, C. *Aspects of Homogenous Catal.* **1988**, *6*, 97. (b) Bhaduri, S.; Gopalkrishnan, K. S.; Clegg, W.; Jones, P. G.; Sheldrick, G. M.; Stalke, D. *J. Chem. Soc., Dalton Trans.* **1984**, 1765. (c) Alper, H.; Hashem, K. E. *J. Am. Chem. Soc.* **1981**, *103*, 6514. (d) DesAbbayes, H.; Alper, H. *J. Am. Chem. Soc.* **1977**, *99*, 98. (e) L'Eplattenier, F.; Matthys, P.; Calderazzo, F. *Inorg. Chem.* **1970**, *9*, 342. (f) Alper, H.; Paik, H. N. *Nouv. J. Chim.* **1978**, *2*, 245. (g) Dawoodi, Z.; Mays, M. J.; Henrick, K. *J. Chem. Soc., Dalton Trans.* **1984**, 433.

(5) (a) Belousov, Yu. A.; Kolosova, T. A. *Polyhedron* **1987**, *6*, 1959. (b) Kunin, A. J.; Noirot, M. D.; Gladfelter, W. L. *J. Am. Chem. Soc.* **1989**, *111*, 2739.

(6) (a) Grate, J. H.; Hamm, D. R.; Valentine, D. H. (Catalytica Associates) U.S. patents 4,705,883 (Nov 10, 1987), 4,629,804 (dec 16, 1986), 4,603,216 (Jul 29, 1986), 4,705,883 (Nov 10, 1987), 4,600,793 (Jul 15, 1986) (b) Grate, J. H.; Hamm, D. R. (Catalytica Associates) U.S. patents 4,687,872 (Aug 18, 1987), 4,709,073 (Nov 24, 1987).

(7) For a preliminary account of part of this work see: Han, S. H.; Geoffroy, G. L.; Rheingold, A. L. *Inorg. Chem.* **1987**, *26*, 3426.

(8) Sappa, E.; Milone, L. *J. Organomet. Chem.* **1973**, *61*, 383.

(9) (a) Lavigne, G.; Kaesz, H. D. *J. Am. Chem. Soc.* **1984**, *106*, 4647. (b) Lavigne, G.; Lugan, N.; Bonnet, J. J. *J. Chem. Soc., Chem. Commun.* **1987**, 957. (c) Han, S. H.; Geoffroy, G. L.; Dombek, B. D.; Rheingold, A. L. *Inorg. Chem.* **1988**, *27*, 4355.

(10) Smieja, J. A.; Gladfelter, W. L. *Inorg. Chem.* **1986**, *25*, 2667.

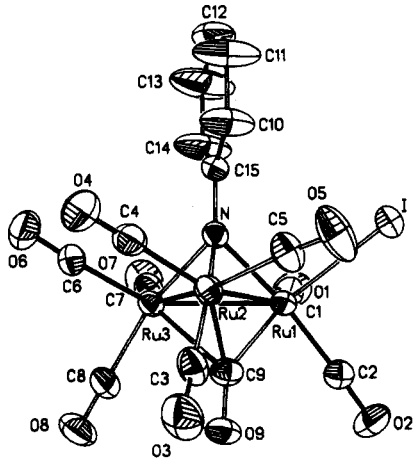

Figure 1. An ORTEP drawing of $[Na(18\text{-crown-}6)][Ru_3(\mu_3\text{-}NPh)(I)(CO)_9]$ (**4c'**). Thermal ellipsoids are drawn at the 40% probability level.

and by chemical analysis. A $[Na(18\text{-crown-}6)]^+$ salt of the iodo derivative **4c** (designated **4c'**) was fully defined by an X-ray diffraction study, the results of which are shown in Figure 1. The structure of the cluster is similar to that of the parent cluster **1**[11] with the iodide having substituted for a CO ligand on a single Ru atom in a position trans to the μ_3-CO. The IR spectra of **4a–d** are similar to that of **4c'**, indicating that all four compounds have similar structures. Noteworthy in each case is the triply bridging carbonyl band in the 1700–1710 cm^{-1} region which is slightly lower in energy than the corresponding band of the parent cluster **1** (1728 cm^{-1}), implying an increase in electron density on the cluster framework caused by the presence of the anionic ligand. The CO_2 formed in the reaction of **3a** with PhNO was identified by IR spectroscopy and by high-resolution mass spectrometry. A similar rapid reaction of nitrosobenzene occurred with the hydrido anion $[HRu_3(CO)_{11}]^-$ to form the known imido cluster **4e**.[12] (eq 6).

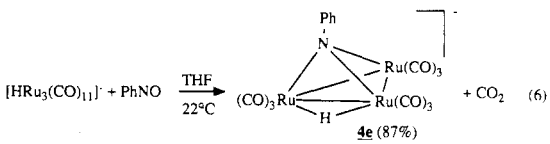

A comparison of the reaction conditions used in eq 4 and 6 to those needed for reaction 3 clearly shows that the presence of halides, cyanide, and hydride ligands in the Ru_3 cluster significantly increases both the rate of reaction and the yields of imido ligands from nitrosobenzene. To put this effect on a quantitative basis, half-lives for the reactions were determined by IR monitoring the disappearance of the starting clusters in THF solution at 22 °C following addition of nitrosobenzene. The observed ordering Cl^- ($t_{1/2}$ < 1 min) ≈ Br^- ($t_{1/2}$ < 1 min) < I^- ($t_{1/2}$ = 15 min) < H^- ($t_{1/2}$ = 40 min) < CN^- ($t_{1/2}$ > 300 min) clearly shows that chloride and bromide are the superior promoters, and the observation that chloride is superior to iodide is exactly that found by Cenini and co-workers[3] in their catalytic studies of nitroaromatic carbonylation (eq 1).

Formation of Imido Clusters via Addition of Nitrosobenzene to Precursors Having a Weakly Coordinated Acetonitrile Ligand. The fact that halides are known promoters for ligand substitution reactions of $Ru_3(CO)_{12}$[9a] suggests that the halide-promoted reactions discussed above could result from the anions promoting substitution of nitrosobenzene for CO with subsequent rapid PhN=O deoxygenation. If so, imido ligands should rapidly form upon addition of nitrosobenzene to $Ru_3(CO)_{11}(NCCH_3)$, a cluster known to readily undergo displacement of the weakly coordinated acetonitrile by other ligands.[13] Indeed, addition of PhNO to solutions of this species resulted in rapid and high-yield formation of the imido cluster $Ru_3(\mu_3\text{-}NPh)(CO)_{10}$ (**1**), and CO_2 (eq 7). A similar reaction occurred to form $Os_3(\mu_3\text{-}NPh)(CO)_{10}$ in 40% yield when $Os_3(CO)_{11}(NCMe)$[14] was treated with PhNO. The cluster $Os_3(\mu_3\text{-}NPh)(CO)_{10}$ has been reported to form in low yield (5%) upon heating PhNO with $Os_3(CO)_{12}$ (octane, 125 °C, 7 h), a reaction that gave the bis(imido) cluster $Os_3(\mu_3\text{-}NPh)_2(CO)_9$ as the major product.[10] The synthetic methodology of eq 7 is clearly the

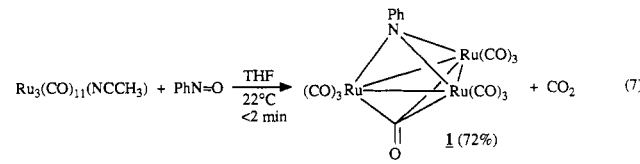

method of choice for the preparation of both $Ru_3(\mu_3\text{-}NPh)(CO)_{10}$ and $Os_3(\mu_3\text{-}NPh)(CO)_{10}$. Attempts were made to try to observe the presumed nitroso-coordinated intermediates in these syntheses by adding PhNO to −78 °C solutions of $Ru_3(CO)_{11}(NCMe)$ and $Os_3(CO)_{11}(NCMe)$, but IR analysis indicated no reaction at this low temperature. As the temperature was increased to −30 °C, the IR spectra showed the formation of the imido clusters $M_3(\mu_3\text{-}NPh)(CO)_{10}$, but without the appearance of other IR bands that could be attributed to an intermediate PhNO substituted species.

This synthetic method was also extended to the preparation of the heteronuclear clusters $FeRu_2(\mu_3\text{-}NPh)(CO)_{10}$ (**5**) and $Fe_2Ru(\mu_3\text{-}NPh)(CO)_{10}$ (**6**) (eq 8 and 9). The ace-

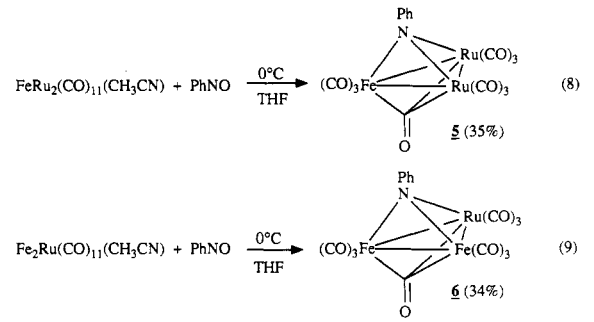

tonitrile-substituted clusters $Fe_2Ru(CO)_{11}(CH_3CN)$ and $FeRu_2(CO)_{11}(CH_3CN)$ have not been previously described, although IR monitoring (see Experimental Section) indicated that they rapidly form upon addition of Me_3NO to acetonitrile solutions of $Fe_2Ru(CO)_{12}$ and $FeRu_2(CO)_{12}$. Addition of nitrosobenzene to solutions of these acetonitrile-substituted clusters led immediately to the new heteronuclear imido species **5** and **6**. The latter were isolated as microcrystalline solids and were spectroscopically characterized. Their mass spectra are consistent with the indicated formulations, and their IR spectra are similar

(11) Bhaduri, S.; Gopalkrishnan, K. S.; Sheldrick, G. A.; Clegg, W.; Stalke, D. *J. Chem. Soc., Dalton Trans.* **1983**, 2339.
(12) Bhaduri, S.; Khwaja, H.; Jones, P. G. *J. Chem. Soc., Chem. Commun.* **1988**, 194.
(13) Foulds, G. A.; Johnson, B. F. G.; Lewis, J. *J. Organomet. Chem.* **1985**, *296*, 147.
(14) (a) Johnson, B. F. G; Lewis, J.; Pippard, D. A. *J. Chem. Soc., Dalton Trans.* **1981**, 407. (b) Shapley, J. R.; Pearson, G. A.; Tachikawa, M.; Schmidt, G. E.; Churchill, M. R.; Hollander, F. J. *J. Am. Chem. Soc.* **1977**, *99*, 8064. (c) Cotton, F. A.; Hanson, B. E. *Inorg. Chem.* **1977**, *16*, 2820.

in band pattern and intensity to that of $Ru_3(\mu_3\text{-NPh})(CO)_{10}$ (**1**), implying similar structures for all three species. Especially important is the respective observation of ν_{CO} bands at 1740 and 1738 cm^{-1} for **5** and **6**, indicating the presence of triply bridging carbonyl ligands as found in the structure of **1** (ν_{CO} = 1728 cm^{-1}).[11] Cluster **5** is similar to the species $FeRu_2(\mu_3\text{-NH})(CO)_{10}$ previously reported by Gladfelter et al. to result from protonation of $[FeRu_3(CO)_{12}]^-$.[15] Small quantities of the bis(imido) cluster $Fe_2Ru(\mu_3\text{-NPh})_2(CO)_9$ (**7**), were occasionally obtained upon chromatography of the reaction mixture from reaction 9 (see Experimental Section). It is significant that the metal composition of the products of reactions 8 and 9 is exactly that of the starting clusters, implying that reaction occurs on the intact heteronuclear clusters with no metal scrambling.

Bis(imido) clusters can also be prepared by an extension of the methodology described above. For example, reaction of the mono(imido) cluster $Ru_3(\mu_3\text{-NPh})(CO)_{10}$ with Me_3NO in the presence of CH_3CN at 22 °C gave immediate formation of a new compound with IR bands at 2086 (w), 2054 (s), 2031 (vs), 2014 (m), and 1709 (w) cm^{-1}. This species is presumably $Ru_3(\mu_3\text{-NPh})(CO)_9(CH_3CN)$, a conclusion supported by the observation that the starting imido cluster $Ru_3(\mu_3\text{-NPh})(CO)_{10}$ was re-formed in quantitative yield upon addition of CO. Addition of either nitrosobenzene or $Bu^tN{=}O$ to solutions of $Ru_3(\mu_3\text{-NPh})(CO)_9(CH_3CN)$ gave immediate formation of the bis(imido) clusters $Ru_3(\mu_3\text{-NPh})_2(CO)_9$ (**2**), and $Ru_3(\mu_3\text{-NPh})(\mu_3\text{-N}^t\text{Bu})(CO)_9$ (**8**), in 49% and 58% respective yields. The formation of compound **8** is particularly significant since it illustrates the use of this methodology to prepare bis(imido) clusters having different substituents on the two imido ligands.

Anion-Promoted Carbonylation of Phenylimido Ligands To Form Phenyl Isocyanate. Imido ligands have proven to be remarkably resistant to carbonylation to form isocyanates. For example, the bis(imido) clusters $Ru_3(\mu_3\text{-NPh})_2(CO)_9$ and $Fe(\mu_3\text{-NPh})_2(CO)_9$ were recovered in 69% (M = Ru) and 89% (M = Fe) yields after heating at 150 °C for 22 h under 120 atm of CO. Similarly, Gladfelter and co-workers found that the mono(imido) cluster $Ru_3(\mu_3\text{-NPh})(CO)_{10}$ (**1**), required high pressure and temperature and a lengthy reaction time to produce PhN=C=O (eq 10).[16] More recently it was found that

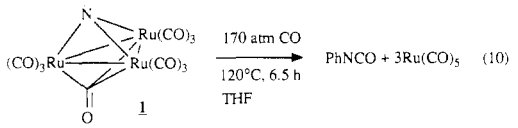

(10)

polar solvents (e.g., CH_3CN) increase the rate of this reaction, although high pressures and temperatures were still required (22 atm, 140 °C).[17] We found that no reaction of **1** with CO occurred under far milder conditions (4 atm, 120 °C, 22 h, THF).

To explore the effect of halides on the imido carbonylation reaction, cluster **1** was allowed to react with halide to form the anions $[Ru_3(\mu_3\text{-NPh})(X)(CO)_9]^-$ described above, and these were then exposed to 1 atm of CO at 22 °C. In each case, a color change occurred over the course of 0.25–3 h as phenyl isocyanate and the anionic clusters $[Ru_3(X)(CO)_n]^-$ formed (eq 11). The isocyanate product was identified by its characteristic IR ν_{CO} band at 2260

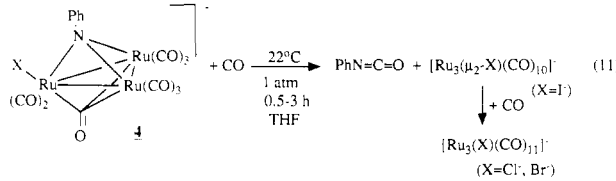

(11)

cm^{-1} and by its conversion to methyl *N*-phenylcarbamate in 45% isolated yield when methanol was added to the solution after reaction.

Infrared monitoring indicated the imido carbonylation reactions to be essentially quantitative, although the rates of the reactions are markedly dependent on the anion attached to the Ru_3 framework. The following order of half-lives was obtained: Cl^- ($t_{1/2}$ = 8 min) < Br^- ($t_{1/2}$ = 80 min) < I^- ($t_{1/2}$ = 5 h) ≪ H^-, CN^- (no reaction) with chloride clearly the superior promoter.

Reaction of the Bis(imido) Cluster $Ru_3(\mu_3\text{-NPh})_2(CO)_9$ (2) with Halides. The bis(imido) cluster $Ru_3(\mu_3\text{-NPh})_2(CO)_9$ also reacts with halides to form the monosubstituted products shown in eq 12. These

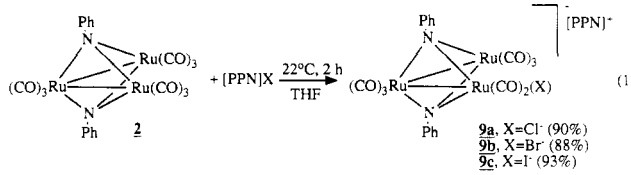

(12)

species were characterized spectroscopically and by chemical analysis, although the specific site of halide substitution was not determined. It is assumed that the halide has added to one of the two equivalent Ru atoms rather than the unique ruthenium, since this is the site in which phosphine substitution has been found to occur in the analogous cluster $Fe_3(\mu_3\text{-NPh})_2(CO)_9$.[18] Halides do not promote the carbonylation of the imido ligands in clusters **9a–c** since these species just lose halide to re-form the parent cluster **2** when placed under CO (1 atm, 22 °C). IR analysis indicated an equilibrium between clusters **2** and **9** with the equilibrium lying in the direction of **9** under these mild conditions. Very slow formation of a small amount of PhNCO occurred over a period of 2 days when solutions of cluster **9c** were maintained under 1 atm of CO.

Preparation of $[CoRu_2(\mu_3\text{-NPh})(CO)_9]^-$ (10) and $HCoRu_2(\mu_3\text{-NPh})(CO)_9$ (11). Several years ago, one of us showed that the anion $[Co(CO)_4]^-$ readily adds to $Ru_3(CO)_{12}$ to form the tetranuclear cluster $[CoRu_3(CO)_{13}]^-$.[19] We had thus anticipated that a *tetranuclear* $CoRu_3$ imido cluster might form by an analogous reaction of $[Co(CO)_4]^-$ with $Ru_3(\mu_3\text{-NPh})(CO)_{10}$. However, when these reagents were heated in refluxing THF, the product proved to be the trinuclear imido cluster $[CoRu_2(\mu_3\text{-NPh})(CO)_9]^-$ (**10**, eq 13). This species was produced by

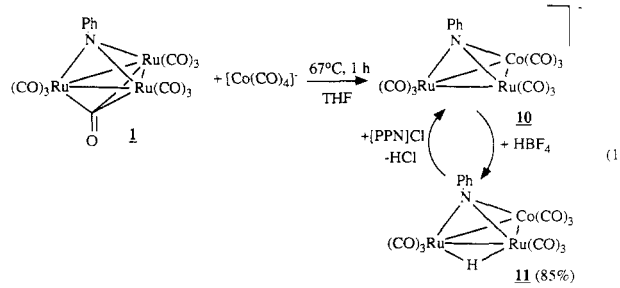

(13)

(15) Blohm, M. L.; Fjare, D. E.; Gladfelter, W. L. *J. Am. Chem. Soc.* **1986**, *108*, 2301.
(16) Smieja, J. A.; Gozum, J. E.; Gladfelter, W. L. *Organometallics* **1987**, *6*, 1311.
(17) Basu, A.; Bhaduri, S.; Khwaja, H. *J. Organomet. Chem.* **1987**, *319*, C28.
(18) (a) Bockman, T. M.; Kochi, J. K. *J. Am. Chem. Soc.* **1987**, *109*, 7725. (b) Kouba, J. K.; Muetterties, E. L.; Thompson, M. R.; Day, V. W. *Organometallics* **1983**, *2*, 1065.
(19) Steinhardt, P. C.; Gladfelter, W. L.; Harley, A. D.; Fox, J. R.; Geoffroy, G. L. *Inorg. Chem.* **1980**, *19*, 332.

a "metal-exchange" reaction of the type that has been used to prepare heteronuclear clusters with capping ligands of all sorts,[20] although imido clusters have never before been made by this method. The anionic cluster **10** proved difficult to isolate in pure form from the above reaction, although it was isolated pure by the alternative procedure described below.

Protonation of solutions of cluster **10** led to the neutral hydride derivative **11** which was isolated in high overall yield from **1** (eq 13). Pure **10** could then be obtained by deprotonation of **11** with [PPN]Cl as also illustrated in the equation. The use of halides as bases for deprotonation of hydride clusters has precedent in other syntheses.[9a] Clusters **10** and **11** have been characterized spectroscopically, and **11** has been fully defined by a crystal structure determination, the results of which are shown in Figure 2 (see below). The phosphinidene analogue of cluster **11**, $HCoRu_2(\mu_3\text{-}PPh)(CO)_9$ (**12**), is a known compound.[20a] As expected, clusters **11** and **12** show similar IR spectra, although the ^1H NMR hydride resonance of **11** (δ −15.7) is ~2 ppm downfield from that of **12** (δ −17.5). The IR spectrum of **10** is similar to that of **11** except that the ν_{CO} bands are shifted to lower energy as a result of the negative charge on the cluster.

Whereas the hydride cluster **11** does not react with CO (150 °C, 7 atm, 24 h), the anionic cluster **10** readily does so to form $[Co(CO)_4]^-$ and $Ru_3(CO)_{12}$ along with the dimer of phenyl isocyanate (**13**) (eq 14). However, no reaction

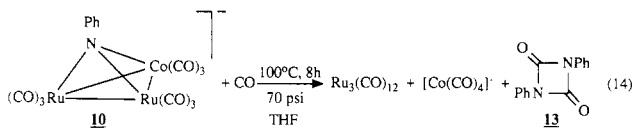

occurred when milder carbonylation conditions were employed (22 °C, 1 atm, 4 h).

Preparation of the Acyl Clusters $[Ru_3(\mu_3\text{-}NPh)(CO)_9(C\{O\}R)]^-$. The acyl-substituted clusters **14** and **15** shown in eq 15 readily form upon addition of the appro-

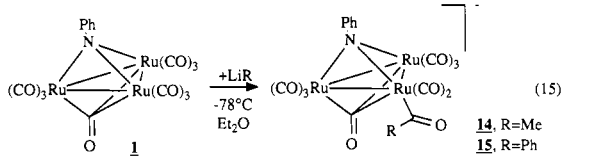

priate lithium reagent to $Ru_3(\mu_3\text{-}NPh)(CO)_{10}$. Clusters **14** and **15** were isolated as yellow solids, although their facile transformation to the amido clusters described below precluded satisfactory elemental analyses. They were typically generated in situ and used for subsequent reactions. Both clusters show weak IR bands at 1680 (**14**) and 1685 cm^{-1} (**15**) indicative of the presence of a triply bridging carbonyl ligand as found in the parent cluster **1**. Cluster **15** shows an acyl ν_{CO} band at 1536 cm^{-1}, but the corresponding band of **14** could not be confidently identified.

Coupling of Acyl and Imido Ligands To Form Amido Clusters. At room temperature, the acyl clusters **14** and **15** slowly transform over a period of days to form the amido clusters **16** and **17** (eq 16). However, these reactions are complete in just 1 h when clusters **14** and **15** are exposed to 1 atm of CO. Addition of tetramethylethylenediamine (TMEDA) to these solutions to complex the Li^+ ion led to the isolation of [Li(TMEDA)]$^+$ salts of **16** and **17** as oily red solids. The IR spectra of these clusters are similar in both band position and intensity to the spectra of $[Ru_3(\mu_2\text{-}Cl)(CO)_{10}]^-$,[9] $[Ru_3(\mu_2\text{-}NCO)(CO)_{10}]$,[21] and $[Ru_3(\mu_2\text{-}O{=}C(NMe_2))(CO)_{10}]^-$[22] which have been established to have structures analogous to that drawn in eq 16 with three μ_2-CO ligands. Particularly indicative of the assigned structure is the presence of two bridging carbonyl bands at 1809 and 1798 cm^{-1}. The acyl carbonyl bands of **16** and **17** were respectively observed at 1530 and 1541 cm^{-1}. As drawn in eq 16, the acyl substituents in **16** and **17** are assumed to be in endo positions with respect to the metal triangle to reflect their migration from the "back" Ru atom to the imido ligand, although there is no spectroscopic data to support this assumption.

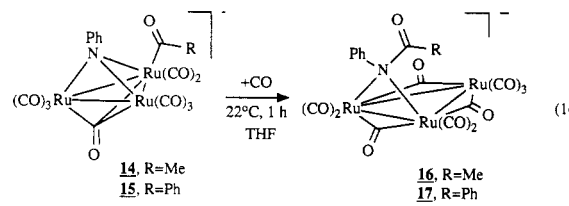

Protonation of $[Ru_3(\mu_2\text{-}NPhC\{O\}R)(CO)_{10}]^-$ To Form $HRu_3(\mu_2\text{-}NPhC\{O\}R)(CO)_{10}$. Clusters **16** and **17** readily undergo protonation to form the neutral hydride derivatives **18** and **19** which were isolated as orange microcrystalline solids (eq 17). The IR spectra of these species are

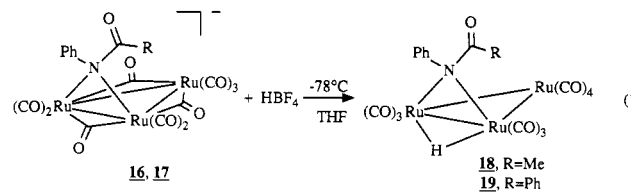

similar to that of the known compound $HRu_3(\mu_2\text{-}NHPh)(CO)_{10}$ which has an edge double-bridged structure like that drawn in eq 17 for **18** and **19**. The acyl bands of **18** and **19** were respectively observed at 1543 and 1550 cm^{-1}, and the ^1H NMR spectra of the two compounds showed the expected hydride resonances at δ −15.02 and −14.06, respectively. It should be noted that when residual CO was present from the previous carbonylation reaction

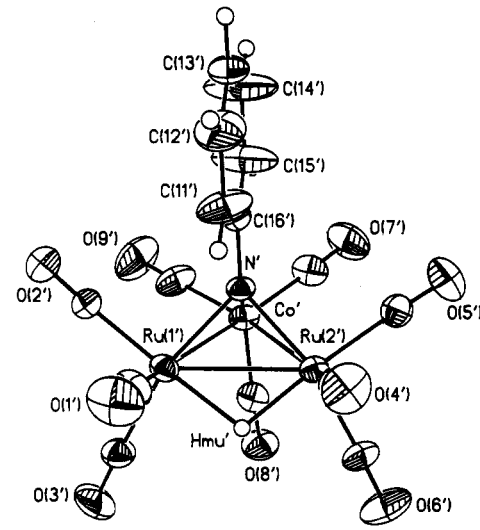

Figure 2. An ORTEP drawing of $HCoRu_2(\mu_3\text{-}NPh)(CO)_9$ (**11**). Thermal ellipsoids are drawn at the 40% probability level.

(20) (a) Mani, D.; Vahrenkamp, H. *Chem. Ber.* **1986**, *119*, 3639. (b) Roberts, D. L.; Geoffroy, G. L. In *Comprehensive Organometallic Chemistry*; Wilkinson, G., Stone, F. G. A., Abel, E. W., Eds.; Pergamon Press: Oxford, 1982; Chapter 40.

(21) Fjare, D. E.; Jensen, J. A.; Gladfelter, W. L. *Inorg. Chem.* **1983**, *22*, 1774.

(22) Mayr, A.; Lin, Y. C.; Boag, N. M.; Kampe, C. E.; Knobler, C. B.; Kaesz, H. D. *Inorg. Chem.* **1984**, *23*, 4640.

Table I. Crystallographic Data for [Na(18-crown-6)][$Ru_3(\mu_3$-NPh)(I)$(CO)_9$] (4c′) and $HCoRu_2(\mu$-NPh$)(CO)_9$ (11)

	4c′	11
	(a) Crystal Parameters	
formula	$Ru_3C_{27}H_{29}INNaO_{15}$	$CoRu_2C_{15}H_6NO_9$
cryst system	triclinic	triclinic
space group	$P\bar{1}$	$P\bar{1}$
a, Å	10.369 (3)	8.609 (2)
b, Å	13.335 (3)	15.547 (4)
c, Å	13.738 (3)	15.721 (4)
α, deg	79.54 (2)	85.07 (2)
β, deg	77.03 (2)	75.97 (2)
γ, deg	86.76 (2)	79.58 (2)
V, Å^3	1820.1 (6)	2005.8 (9)
Z	2	4
D(calcd), g cm^{-3}	1.935	2.004
μ(Mo Kα), cm^{-1}	21.3	23.2
temp, °C	21	23
size, mm	0.28 × 0.28 × 0.36	0.36 × 0.36 × 0.39
color	red	orange
	(b) Data Collection	
diffractometer	Nicolet R3m	
radiatn	Mo Kα	
wavelength, Å	0.710 73	
monochromator	graphite	
scan method	Wyckoff	
scan limits, deg	$4 \le 2\theta \le 52$	$4 \le 2\theta \le 48$
octants collected	$\pm h,\pm k,\pm l$	
std rflns	3 std/97 reflns	
decay	<1%	<2%
rflns collected	7476	6550
indpdt rflns	7176	6137
obsd rflns	5663 ($4\sigma(F_o)$)	5172 ($3\sigma(F_o)$)
R(int), %	2.12	2.21
	(c) Data Reduction and Refinement	
$R(F)$, %	4.55	4.17
R(wF), %	5.20 (g = 0.001)[a]	5.26 (g = 0.001)[a]
GOF	1.492	1.118
Δ/σ (last cycle)	0.08	0.93
N_o/N_v	12.6	9.9
$\Delta(\rho)$, e Å^{-3}	1.19	0.93

[a] $R(F) = \sum(||F_o| - |F_c||)/\sum|F_o|$; $R(wF) = \sum(w^{1/2}(||F_o| - |F_c||))/(w^{1/2}|F_o|)$; GOF = $[\sum w||F_o| - |F_c||/(N_o - N_v)]^{1/2}$; $w^{-1} = \sigma^2(F_o) + gF_o^2$.

(e.g., 14 → 16), the isolated yields of 18 and 19 were lowered due to their ready carbonylation to form free amides and the hydride cluster $H_2Ru_4(CO)_{13}$, as discussed below.

Carbonylation of $HRu_3(\mu_2$-NPhC{O}Me$)(CO)_{10}$ To Release Acetanilide. Bhaduri and co-workers have shown that aniline readily formed upon carbonylation (10 atm, 30 °C) of $H_2Ru_3(\mu_3$-NPh$)(CO)_9$.[4b] Similarly, we found that acetanilide was readily released from cluster 18 when it was treated with CO under the mild conditions shown in eq 18. IR analysis indicated this reaction to be quantitative, although the isolated yields of the products were considerably lower.

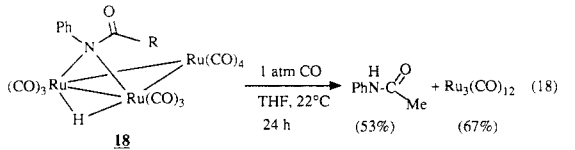

18

Crystal and Molecular Structure of [Na(18-crown-6)][$Ru_3(\mu_3$-NPh)(I)$(CO)_9$] (4c′). The PPN^+ salts of **4a–d** failed to give crystals suitable for an X-ray diffraction study although such a crystal was obtained for the $[Na(18\text{-crown-6})]^+$ salt of **4c** (designated **4c′**). An ORTEP drawing of the cluster anion is shown in Figure 1, and relevant crystallographic parameters are set out in Tables I–III. The cluster anion consists of a triangular Ru_3 core capped by μ_3-imido and μ_3-carbonyl ligands. The iodide is terminally bonded to one Ru atom in a position trans

Table II. Atomic Coordinates (×10^4) and Isotropic Thermal Parameters (Å^2 × 10^3) for [Na(18-crown-6)][$Ru_3(\mu_3$-NPh)(I)$(CO)_9$] (4c′)

	x	y	z	U[a]
I	2485.1 (5)	6983.2 (4)	1076.7 (4)	74 (1)*
Ru(1)	3193.6 (5)	8339.1 (4)	2157.3 (4)	47 (1)*
Ru(2)	943.1 (5)	8385.2 (4)	3682.6 (4)	51 (1)*
Ru(3)	3367.8 (5)	8515.3 (4)	4079.5 (4)	51 (1)*
N	2582 (5)	7408 (4)	3536 (4)	50 (2)*
O(1)	6100 (5)	7899 (5)	1497 (5)	101 (3)*
O(2)	3444 (6)	10058 (4)	336 (4)	97 (3)*
O(3)	−786 (7)	10288 (5)	3851 (5)	112 (3)*
O(4)	−449 (7)	7529 (5)	5866 (5)	109 (3)*
O(5)	−860 (6)	7579 (6)	2520 (6)	119 (4)*
O(6)	2556 (7)	7597 (5)	6307 (4)	109 (3)*
O(7)	6286 (6)	7934 (5)	3894 (6)	108 (3)*
O(8)	3756 (7)	10592 (4)	4585 (5)	109 (3)*
O(9)	2336 (5)	10424 (3)	2696 (4)	72 (2)*
C(1)	5030 (7)	8033 (6)	1751 (5)	67 (3)*
C(2)	3381 (7)	9383 (6)	1021 (6)	64 (3)*
C(3)	−157 (8)	9567 (6)	3794 (6)	72 (3)*
C(4)	85 (7)	7828 (5)	5056 (6)	71 (3)*
C(5)	−175 (7)	7835 (6)	2954 (6)	74 (3)*
C(6)	2850 (8)	7971 (6)	5477 (6)	71 (3)*
C(7)	5202 (7)	8142 (6)	3932 (6)	67 (3)*
C(8)	3628 (8)	9825 (6)	4398 (6)	72 (3)*
C(9)	2385 (6)	9529 (5)	2867 (6)	62 (3)*
C(10)	1533 (4)	5775 (4)	3964 (6)	119 (6)*
C(11)	1605	4716	4231	163 (8)*
C(12)	2813	4235	4321	122 (6)*
C(13)	3949	4812	4145	200 (11)*
C(14)	3877	5871	3878	145 (7)*
C(15)	2669	6352	3788	58 (3)*
Na	2084 (3)	7034 (3)	−1526 (3)	102 (2)*
O(10)	1446 (14)	8852 (10)	−1476 (9)	273 (9)*
O(11)	3760 (12)	8361 (10)	−2082 (12)	238 (9)*
O(12)	4278 (9)	6337 (10)	−1698 (8)	209 (7)*
O(13)	2284 (17)	4959 (9)	−1119 (10)	282 (10)*
O(14)	525 (12)	6072 (10)	−2204 (9)	206 (7)*
O(15)	−327 (7)	7222 (10)	−734 (8)	215 (6)*
C(16)	2570 (15)	9553 (8)	−1908 (11)	188 (9)*
C(17)	4028 (18)	8980 (17)	−1872 (15)	241 (13)*
C(18)	5134 (15)	7807 (15)	−2242 (17)	278 (14)*
C(19)	5185 (14)	6852 (20)	−1688 (15)	272 (15)*
C(20)	4244 (21)	5198 (16)	−1223 (17)	291 (14)*
C(21)	3478 (24)	4845 (22)	−2188 (22)	394 (22)*
C(22)	953 (30)	4658 (19)	−1495 (19)	333 (19)*
C(23)	1181 (29)	5134 (13)	−2368 (16)	386 (19)*
C(24)	−848 (15)	6111 (17)	−1599 (15)	222 (12)*
C(25)	−1171 (12)	7401 (14)	−1239 (16)	229 (12)*
C(26)	−424 (16)	8400 (12)	−415 (16)	184 (10)*
C(27)	491 (24)	9093 (18)	−1208 (14)	252 (14)*

[a] Parameters with an asterisk are equivalent isotropic U defined as one-third of the trace of the orthogonalized U_{ij} tensor.

to the μ_3-CO ligand. When compared to the structure of the unsubstituted parent cluster 1,[11] the only notable structural consequence of the halide substitution is the movement of the μ_3-CO closer to Ru(1) {Ru(1)–C(9) = 2.053 (7) Å} which has the iodide attached and away from Ru(2) {Ru(2)–C(9) = 2.168 (6) Å}. There is no significant change in the Ru–Ru {$(Ru\text{–}Ru)_{av}$ = 2.740 Å} and Ru–N {$(Ru\text{–}N)_{av}$ = 2.062 Å} distances as compared to 1 {$(Ru\text{–}Ru)_{av}$ = 2.746 Å; $(Ru\text{–}N)_{av}$ = 2.053 Å}.

The cation in the structurally characterized salt is $[Na(18\text{-crown-6})]^+$, and as typically occurs, complexation of a "too-small" Na^+ ion by 18-crown-6 produces much greater distortion in the polyether than found in highly symmetrical K^+ complexes. The Na^+ ion forms five ether associations in the range 2.39 (1)–2.54 (1) Å and a sixth, longer one at 2.73 Å. The Na^+ ion also is axially associated with the iodine atom and with a terminal carbonyl oxygen O(6) via an isocarbonyl link. These relationships are shown in the unit-cell packing diagram given in Figure 3. The Na^+–O(6) interaction is long and its presence appears to

Table III. Selected Bond Distances and Angles for [Na(18-crown-6)][$Ru_3(\mu_3$-NPh)(I)$(CO)_9$] (4c′)

(a) Anion Bond Distances (Å)

Ru(1)–Ru(2)	2.770 (1)	Ru(2)–C(5)	1.941 (9)
Ru(1)–Ru(3)	2.740 (1)	Ru(3)–C(6)	1.892 (7)
Ru(2)–Ru(3)	2.711 (1)	Ru(3)–C(7)	1.914 (7)
Ru(1)–I	2.762 (1)	Ru1(3)–C(8)	1.923 (8)
N–Ru(1)	2.056 (5)	C(1)–O(1)	1.101 (8)
N–Ru(2)	2.077 (5)	C(2)–O(2)	1.171 (9)
N–Ru(3)	2.052 (6)	C(3)–O(3)	1.136 (11)
C(9)–Ru(1)	2.053 (7)	C(4)–O(4)	1.136 (9)
C(9)–Ru(2)	2.168 (6)	C(5)–O(5)	1.126 (12)
C(9)–Ru(3)	2.329 (7)	C(6)–O(6)	1.138 (9)
Ru(1)–C(1)	1.903 (7)	C(7)–O(7)	1.134 (9)
Ru(1)–C(2)	1.876 (7)	C(8)–O(8)	1.120 (11)
Ru(2)–C(3)	1.901 (8)	C(9)–O(9)	1.175 (8)
Ru(2)–C(4)	1.928 (7)		

(b) Cation Bond Distances (Å)

Na–I	3.680 (5)	Na–O(12)	2.386 (10)
Na···O(6)	2.871 (7)	Na–O(13)	2.727 (12)
Na–O(10)	2.486 (13)	Na–O(14)	2.543 (15)
Na–O(11)	2.448 (13)	Na–O(15)	2.512 (8)

(c) Anion Bond Angles (deg)

Ru(1)–Ru(2)–Ru(3)	60.02 (4)	Ru(1)–C(1)–O(1)	177.0 (7)
Ru(2)–Ru(3)–Ru(1)	61.08 (4)	Ru(1)–C(2)–O(2)	176.7 (6)
Ru(3)–Ru(1)–Ru(2)	58.90 (3)	Ru(2)–C(3)–O(3)	178.2 (7)
Ru(1)–N–Ru(2)	84.2 (2)	Ru(2)–C(4)–O(4)	177.6 (7)
Ru(1)–N–Ru(3)	83.7 (2)	Ru(2)–C(5)–O(5)	175.4 (7)
Ru(2)–N–Ru(3)	82.1 (2)	Ru(3)–C(6)–O(6)	176.7 (7)
Ru(1)–N–C(15)	129.4 (4)	Ru(3)–C(7)–O(7)	176.3 (8)
Ru(2)–N–C(15)	130.4 (3)	Ru(3)–C(8)–O(8)	178.7 (8)
Ru(3)–N–C(15)	129.7 (5)	Ru(1)–C(9)–O(9)	139.1 (5)
Ru(1)–C(9)–Ru(2)	82.0 (2)	Ru(2)–C(9)–O(9)	132.8 (5)
Ru(1)–C(9)–Ru(3)	77.1 (2)	Ru(3)–C(9)–O(9)	126.8 (6)
Ru(2)–C(9)–Cu(3)	74.0 (2)		

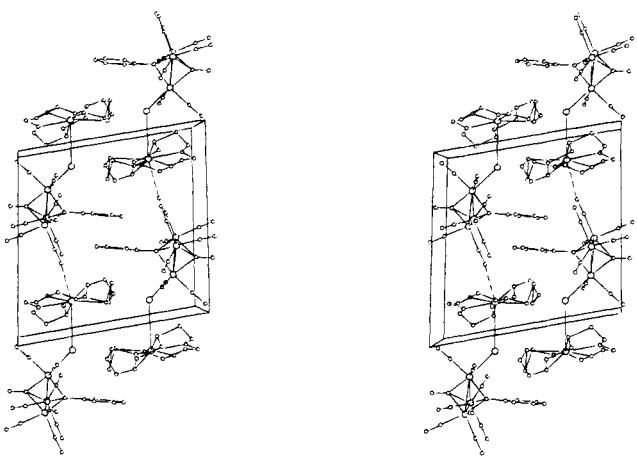

Figure 3. A stereoview of the unit-cell packing diagram for 4c′ viewed down the *a* axis.

be without effect on the C–O or Ru–C distances for the C(6)–O(6) carbonyl.

Crystal and Molecular Structure of $HCoRu_2(\mu_3$-NPh)$(CO)_9$ (11). Cluster 11 crystallizes in the space group $P\bar{1}$ with two independent molecules in the asymmetric unit. One of these is ordered, but the other is disordered over the metal atoms Ru(2) and Co such that each site is approximately one-third the character of the other. An ORTEP drawing of the ordered molecule is shown in Figure 2. The structure of the disordered molecule is similar, except that a low-occupancy (~20%) μ_3-CO ligand is located on the opposite side of the metal plane from the μ_3-NPh group. The hydride ligand in the ordered molecule was located and refined. The important crystallographic parameters are given in Tables I, IV, and V.

The imido ligand symmetrically caps the Ru_2Co triangle with little variation in M′–N′ distances (1.927–2.043 Å) and

Table IV. Atomic Coordinates (×10^4) and Isotropic Thermal Parameters (Å^2 × 10^3) for $HCoRu_2(\mu_3$-NPh$)(CO)_9$ (11)

	x	*y*	*z*	U^a
Ru(1)	1535 (1)	4228 (1)	6739 (1)	47 (1)*
Ru(2)	2525 (1)	2724 (1)	7645 (1)	47 (1)*
Co	4695 (1)	3534 (1)	6549 (1)	46 (1)*
N	2972 (6)	3963 (3)	7625 (3)	43 (2)*
C(1)	−583 (10)	4569 (6)	7496 (6)	75 (3)*
O(1)	−1799 (8)	4722 (5)	7940 (5)	115 (3)*
C(2)	1828 (10)	5420 (5)	6404 (5)	66 (3)*
O(2)	2038 (8)	6105 (3)	6175 (4)	91 (3)*
C(3)	656 (11)	4075 (5)	5749 (6)	75 (4)*
O(3)	188 (11)	3983 (4)	5174 (5)	125 (4)*
C(4)	2547 (13)	1601 (7)	7182 (8)	76 (5)*
C(4A)	2176 (63)	2162 (33)	6884 (35)	98 (15)*
O(4)	2579 (12)	986 (7)	9850 (9)	141 (6)*
O(4A)	2253 (39)	1723 (23)	6232 (22)	87 (11)*
C(5)	593 (12)	2657 (5)	8497 (6)	81 (4)*
O(5)	−599 (9)	2659 (5)	8997 (5)	121 (4)*
C(6)	3897 (13)	2196 (6)	8334 (6)	89 (4)*
O(6)	4761 (13)	1824 (6)	8757 (6)	151 (5)*
C(7)	5576 (11)	4500 (6)	6037 (5)	78 (4)*
O(7)	6137 (9)	5087 (4)	5711 (4)	101 (3)*
C(8)	6390 (11)	3037 (6)	7029 (6)	83 (4)*
C(9)	4569 (22)	2978 (9)	5686 (9)	76 (7)*
C(9A)	5897 (26)	2849 (11)	5447 (15)	65 (8)*
O(8)	7452 (9)	2720 (5)	7323 (6)	126 (4)*
O(9)	4520 (15)	2588 (7)	5116 (7)	104 (6)*
O(9A)	6363 (20)	2418 (9)	4868 (9)	95 (7)*
C(11)	2257 (8)	4339 (4)	9156 (4)	112 (6)*
C(12)	2309	4872	9815	127 (6)*
C(13)	3181	5566	9610	103 (5)*
C(14)	3999	5727	8746	91 (4)*
C(15)	3946	5194	8087	81 (4)*
C(16)	3075	4500	8292	46 (2)*
C(17)	2956 (42)	2896 (22)	6192 (23)	53 (9)
O(17)	2846 (28)	2474 (15)	5604 (15)	59 (7)
Ru(1′)	153 (1)	1807 (1)	2260 (1)	49 (1)*
Ru(2′)	1802 (1)	1691 (1)	3594 (1)	44 (1)*
Co′	1240 (1)	330 (1)	2970 (1)	48 (1)*
N′	2428 (6)	1229 (3)	2370 (3)	44 (2)*
C(1′)	269 (10)	2998 (6)	1793 (6)	74 (3)*
O(1′)	355 (10)	3664 (4)	1553 (5)	121 (4)*
C(2′)	364 (9)	1368 (6)	1126 (5)	73 (4)*
O(2′)	574 (8)	1137 (5)	450 (4)	109 (3)*
C(3′)	−2191 (9)	2016 (5)	2584 (5)	66 (3)*
O(3′)	−3554 (7)	2123 (5)	2804 (5)	112 (3)*
C(4′)	2534 (10)	2809 (5)	3446 (5)	63 (3)*
O(4′)	2945 (8)	3458 (4)	3317 (5)	98 (3)*
C(5′)	3682 (10)	1087 (5)	3978 (5)	63 (3)*
O(5′)	4756 (8)	742 (4)	4236 (5)	101 (3)*
C(6′)	536 (10)	1853 (5)	4772 (5)	67 (3)*
O(6′)	−270 (10)	1922 (4)	5466 (4)	112 (3)*
C(7′)	2680 (10)	−471 (5)	3383 (5)	69 (3)*
O(7′)	3567 (8)	−1002 (4)	3633 (5)	109 (4)*
C(8′)	−532 (9)	351 (4)	3839 (5)	59 (3)*
O(8′)	−1629 (7)	329 (4)	4412 (4)	81 (3)*
C(9′)	850 (12)	−298 (6)	2173 (6)	79 (4)*
O(9′)	587 (11)	−760 (5)	1710 (5)	129 (4)*
C(11′)	4392 (7)	1954 (3)	1295 (4)	99 (4)*
C(12′)	5824	1906	642	124 (6)*
C(13′)	6751	1093	405	96 (5)*
C(14′)	6246	328	821	196 (9)*
C(15′)	4814	377	1475	139 (6)*
C(16′)	3887	1190	1712	53 (3)*
Hmu′	−1 (62)	2171 (32)	3350 (34)	32 (14)

[a] Parameters with an asterisk are equivalent isotropic *U* defined as one-third of the trace of the orthogonalized U_{ij} tensor.

M′–N′–C(16′) angles (127.2°–131.8°). The Ru′–Co′ distances of 2.586 and 2.575 Å are slightly shorter than Ru–Co bond lengths in other compounds ($[CoRu_3(CO)_{13}]^-$, Co–Ru_{av} = 2.618 Å;[19] $H_3CoRu_3(CO)_{12}$, Co–Ru_{av} = 2.675 Å[23]), but the Ru(1′)–Ru(2′) bond length of 2.781 (1) Å is sig-

(23) Gladfelter, W. L.; Geoffroy, G. L.; Calabrese, J. C. *Inorg. Chem.* **1983**, *19*, 2569.

Table V. Important Bond Lengths and Angles for the Completely Ordered of the Two Independent Molecules of $HCoRu_2(\mu_3\text{-}NPh)(CO)_9$ (11)

(a) Bond Distances (Å)

Ru(1′)-Ru(2′)	2.781 (1)	Ru(2′)-C(4′)	1.930 (8)
Ru(1′)-Co′	2.586 (1)	Ru(2′)-C(5′)	1.922 (8)
Ru(2′)-Co′	2.575 (1)	Ru(2′)-C(6′)	1.920 (7)
R1(1′)-N′	2.043 (5)	Co′-C(7′)	1.789 (8)
Ru(2′)-N′	2.025 (5)	Co′-C(8′)	1.782 (7)
Co′-N′	1.927 (5)	Co′-C(9′)	1.780 (10)
Ru(1′)-C(1′)	1.942 (9)	Ru(1′)-H(μ′)	1.82 (6)
Ru(1′)-C(3′)	1.932 (7)	Ru(2′)-H(μ′)	1.71 (5)

(b) Bond Angles (deg)

Ru(1′)-Ru(2′)-Co′	57.59 (4)	C(2′)-Ru(1′)-C(3′)	96.5 (4)
Ru(2′)-(Co′)-Ru(1′)	65.22 (5)	N′-Ru(2′)-C(4′)	104.4 (3)
Co′-Ru(1′)-Ru(2′)	57.23 (5)	N′-Ru(2′)-C(5′)	97.0 (3)
Ru(1′)-N′-Ru(2′)	86.2 (2)	N′-Ru(2′)-C(6′)	156.7 (3)
Ru(1′)-N′-Co′	81.2 (2)	C(4)-Ru(2′)-C(5′)	93.8 (4)
Ru(2′)-N′-Co′	81.3 (2)	C(4′)-Ru(2′)-C(6′)	95.9 (3)
N′-Co′-Ru(1′)	51.3 (1)	C(5′)-Ru(2′)-C(6′)	93.0 (3)
N′-Co′-Ru(2′)	51.0 (2)	N′-Co′-C(7′)	105.9 (3)
N′-Ru(1′)-Ru(2′)	46.6 (1)	N′-Co′-C(8′)	132.8 (3)
N′-Ru(1′)-Co′	47.4 (1)	N′-Co′-C(9′)	108.6 (3)
N′-Ru(2′)-Ru(1′)	47.1 (1)	C(7′)-Co′-C(8′)	102.1 (4)
N′-Ru(2′)-Co′	47.7 (2)	C(7′)-Co′-C(9′)	99.2 (4)
N′-Ru(1′)-C(1′)	107.9 (3)	C(8′)-Co′-C(9′)	103.3 (4)
N′-Ru(1′)-C(2′)	94.7 (3)	Ru(1′)-H(μ′)-Ru(2′)	104 (2)
N′-Ru(1′)-C(3′)	155.5 (3)	all M-C-O	≥175
C(1′)-Ru(1′)-C(2′)	93.2 (4)	C(1′)-Ru(1′)-C(3′)	93.2 (3)

nificantly shorter than a typical Ru–Ru bond bridged by a hydride ligand ($H_3CoRu_3(CO)_{12}$, $Ru\text{-}Ru_{av}$ = 2.898 Å[23]).

Discussion

One important objective of the work described herein was to evaluate the effect of halides on the mechanistic steps outlined in Scheme I so as to provide possible insight into the role that halides play in the promotion of nitroaromatic carbonylation catalysis.[3] The data presented herein clearly show that halides promote both the formation of imido ligands from nitrosobenzene and their carbonylation to form phenyl isocyanate, two of the important steps illustrated in Scheme I. The former effect is best illustrated by the comparison of the reactivity of $Ru_3(CO)_{12}$ with nitrosobenzene in the presence and absence of halides. In the absence of halides, this species slowly reacts at elevated temperature with PhNO to form $Ru_3(\mu_3\text{-}NPh)(CO)_{10}$ in modest yield (eq 3).[10] However, when halides are present, the reaction is complete within minutes at room temperature to give near quantitative yields of the halide-substituted clusters $[Ru_3(\mu_3\text{-}NPh)(X)(CO)_9]^-$. Since halides are known to rapidly react with $Ru_3(CO)_{12}$ to form the anionic clusters $[Ru_3(X)(CO)_n]^-$ (n = 10, 11),[9] these latter species must be the key intermediates in the imido-forming reaction. Indeed, as detailed above, these individual anionic clusters were found to rapidly react with PhNO to form the imido products with a reactivity ordering $Cl^- > Br^- > I^-$.

Halides are of course promoters for many catalytic reactions,[24] but one process of relevance to the work described herein is the halide promotion of substitution reactions of $Ru_3(CO)_{12}$.[9a] For example, Kaesz and Lavigne have shown that whereas $Ru_3(CO)_{12}$ does not react with PPh_3 at room temperature, the presence of catalytic amounts (<5%) of halides induces rapid substitution to form $Ru_3(CO)_{11}(PPh_3)$.[9a] Clearly the role of the halides must be to labilize a CO ligand, although it is not known exactly how they accomplish this function.[25] The halide promoting ability for these substitution reactions was found to be Cl > Br > I,[9a] which is similar to that found in this work.

Scheme II

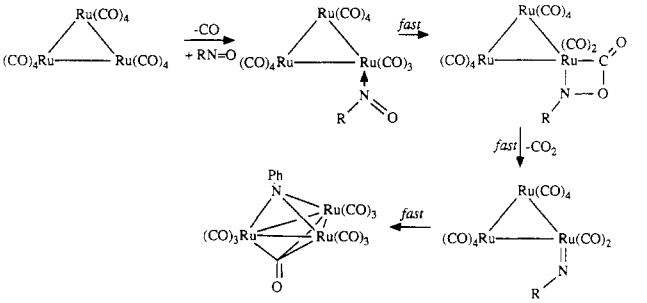

Scheme III

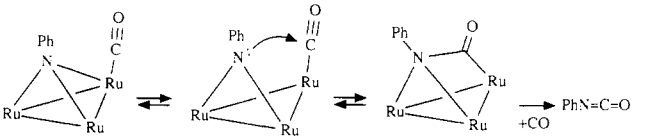

We suggest that the effect of halides in the nitrosobenzene to imido conversion is the same as in the halide-catalyzed substitution reactions studied by *Kaesz and Lavigne*,[9a] *namely, to labilize a CO ligand and open a coordination site for nitrosobenzene to bind.* Once coordinated, rapid deoxygenation must ensue to form the imido ligand via the sequence of steps illustrated in Scheme II. If this explanation is correct, then other methods of opening coordination sites on the $Ru_3(CO)_{12}$ cluster should have the same effect. This is indeed so as illustrated by reaction 7 in which the lightly stabilized cluster $Ru_3(CO)_{11}(CH_3CN)$[13] was shown to *rapidly* react with PhNO at 22 °C to form the imido cluster $Ru_3(\mu_3\text{-}NPh)(CO)_{10}$ in the highest yield thus far reported for this species. Similar methodology was also used to prepare $FeRu_2$, Fe_2Ru, and Os_3 imido clusters as well as $Ru_3(\mu_3\text{-}NPh)(\mu_3\text{-}NBu^t)(CO)_9$. The presumed intermediate shown in Scheme II having a coordinated nitroso ligand was not observed, even at low temperature, implying that once the nitrosobenzene coordinates it rapidly undergoes the deoxygenation reaction, presumably by formation of a metallacycle leading to a metathesis-type reaction. Further support for the proposal that halides promote the imido-forming reaction by promoting substitution of a nitroso ligand for CO comes from the facile reaction of $[HRu_3(CO)_{11}]^-$ with PhN=O to form the imido cluster $[HRu_3(\mu_3\text{-}NPh)(CO)_9]^-$ (eq 6) since $[HRu_3(CO)_{11}]^-$ has been shown to exhibit a greatly enhanced rate of substitution as compared to $Ru_3(CO)_{12}$.[26]

The results reported herein also show that halides dramatically accelerate the carbonylation of imido ligands to form phenyl isocyanate. This is well illustrated by the conditions needed to force the carbonylation in the absence of halide (170 atm of CO, 120 °C, 6.5 h)[16] and when halides are present (1 atm of CO, 22 °C, 1 h). There are few reported examples of the formation of phenyl isocyanate from the carbonylation of imido ligands, but the limited data suggest the generalized mechanism shown in Scheme III for trinuclear clusters. The first step likely involves

(24) (a) Dombek, B. D. *J. Organomet. Chem.* **1983**, *250*, 467. (b) Dombek, B. D. *J. Am. Chem. Soc.* **1981**, *103*, 6508. (c) Dombek, B. D. *Europ. Pat. Appl.* **1979**, 0013008. (d) Dombek, B. D. *Organometallics* **1985**, *4*, 1707. (e) Knifton, J. F. *J. Am. Chem. Soc.* **1981**, *103*, 3959. (f) Knifton, J. F. *J. Mol. Catal.* **1981**, *11*, 91. (g) Yoshida, S. I.; Mori, S.; Kinoshita, H.; Watanabe, Y. *J. Mol. Catal.* **1987**, *42*, 215. (h) Hidai, M.; Koyasu, Y.; Chikanari, K.; Uchida, Y. *J. Mol. Catal.* **1987**, *40*, 243.

(25) For a discussion of the possible mechanism of this process, see: Lavigne, G.; Kaesz, H. D. In *Metal Clusters in Catalysis*; Knozinger, H., Gates, B. C., Guczi, L., Eds.; Elsevier: Amsterdam, 1986; pp 68–69.

(26) (a) Taube, D. J.; Ford, P. C. *Organometallics* **1986**, *5*, 99. (b) Lavigne, G.; Lugan, N.; Bonnet, J. J. *Inorg. Chem.* **1987**, *26*, 2345.

Scheme IV

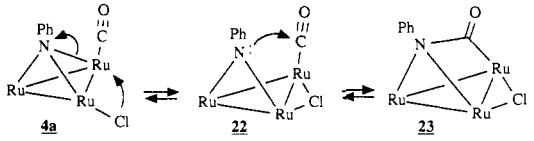

dissociation of the triply bridging imido ligand from one of the metal atoms to form a dibridging imido ligand. Like basic amines, this μ_2-imido ligand should nucleophilically attack a CO ligand to form a coordinated phenyl isocyanate. Displacement of this ligand by added CO would then give the free isocyanate.

Strong support for these suggestions comes from the recent work of Bhaduri and co-workers[12] who showed that deprotonation of the amido ligand of $HRu_3(\mu_2\text{-}NHPh)(CO)$ (**20**) gave formation of cluster **21** (eq 19) which was

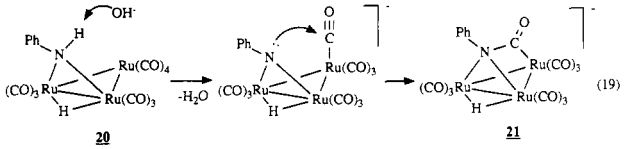

(19)

structurally characterized and shown to have a coordinated phenyl isocyanate ligand. It was suggested that this reaction proceeded by deprotonation of the amido ligand to generate a nucleophilic μ_2-imido ligand that then attacked a CO. Similarly, Deeming and co-workers[27] proposed the intermediacy of a species with a basic μ_2-imido ligand to account for the formation of the isocyanate complex $HOs_3(CO)_8(L)\{Bu^tCH{=}NN{=}C{=}O\}$ from the reaction of $H_2Os_3(CO)_9(L)$ (L = CO, PM_2Ph) with Bu^tCHN_2. Sharp and co-workers[28] have also implicated a similar mechanism for a reaction involving the carbonylation of an imido ligand on a dirhodium complex.

There thus seems little doubt that the isocyanate forming reaction proceeds as illustrated in Scheme III, but still to be resolved is how halides promote this transformation. Presumably halides labilize one of the three Ru–N bonds to accelerate the formation of the nucleophilic μ_2-imido ligand. This could result just from the increased negative charge on the cluster which should weaken the dative interaction between the imido ligand and a ruthenium atom. Support for this suggestion comes from a comparison of the carbonylation behavior of $HCoRu_2(\mu_3\text{-}NPh)(CO)_9$ (**11**) and $[CoRu_2(\mu_3\text{-}NPh)(CO)_9]^-$ (**10**) described above. The neutral hydride cluster **11** is resistant to carbonylation whereas the anionic cluster **10** readily carbonylates under mild conditions, implying that the increased electron density on **10** as compared to **11** activates the cluster toward carbonylation. However, the observation that the anionic clusters $[Ru(\mu_3\text{-}NPh)(CN)(CO)_9]^-$ and $[HRu(\mu_3\text{-}NPh)(CO)_9]^-$ do not carbonylate, whereas the corresponding halide substituted clusters **4a–c** do, indicates that there is more involved than just an increase in electron density, and some special effect must be associated with halides.

Halides could promote the carbonylation reaction by moving to a bridging position and displacing one of the Ru–N bonds as illustrated in Scheme IV. Each of the clusters illustrated in this scheme has exactly the same electron count, and it is conceivable that they are in equilibrium. If so, the equilibrium must lie far to the left since solutions of **4a** in the absence of CO showed only IR bands attributable to this complex. The suggested

Scheme V

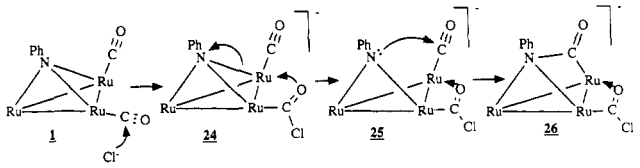

Scheme VI

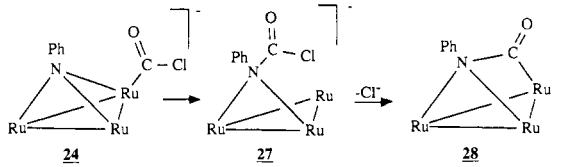

mechanism of Scheme IV is consistent with the observation that clusters **4d** (X = CN) and **4e** (X = H) do not readily carbonylate since cyanide rarely assumes a bridging position and the hydride ligand, which can only be a two-electron donor, is already in a bridging position in cluster **4e**.

A less likely explanation of the halide effect would involve nucleophilic attack of halide on a coordinated CO to form a haloacyl ligand as in **24** (Scheme V). This species could then labilize one of the Ru–N bonds by assuming a bridging position (**25**), and the μ_2-imido ligand could then attack a CO to form the coordinated isocyanate. Alternatively, labilization of one of the Ru–N bonds could occur as a consequence of the increased electron density on the cluster, thereby weakening the N→Ru dative interaction. It is also possible that the chloroacyl ligand could migrate to the imido ligand as illustrated in Scheme VI to form **27**. Loss of chloride from this species would give a coordinated isocyanate complex. The chloroacyl–imido coupling reaction finds support in the acyl–imido coupling results described above. However, while the intermediacy of a species like **24** cannot be ruled out, there is little precedence for the formation of haloacyl ligands,[29] and we thus view these mechanisms as unlikely.

The results described above in eq 15–18 show that acyl ligands can migrate to imido ligands and that free anilides can be formed from the resultant amido clusters. These reactions effectively model the other suggested route to carbamate products that is outlined in Scheme I. These reactions complement the earlier observations that thermolysis or oxidation of the methoxycarbonyl and acyl clusters $[Fe_3(\mu_3\text{-}NPh)_2(CO)_8(C\{O\}R)]^-$ (R = OMe, Ph) led to the formation of methyl *N*-phenylcarbamate and benzanilide, respectively.[30] Furthermore, we believe the acyl–imido coupling reactions to be closely related to the carbene–imido and carbene–phosphinidene coupling reactions discovered earlier in these laboratories that are illustrated in eq 20.[30] With cluster **29a**, carbene–imido

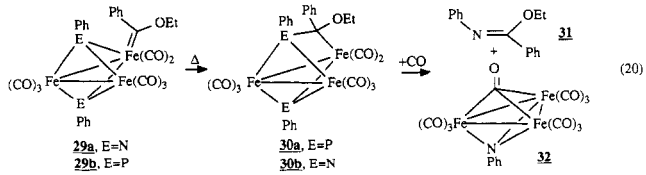

(20)

coupling occurred to produce the free imidate **31**, but with **29b**, this reaction stopped at the intermediate stage (**30a**) with the PhP=C(OEt)Ph ligand still attached to the metal framework. Since carbene and acyl ligands are isolobal,

(27) Deeming, A. J.; Fuchita, Y.; Hardcastle, K.; Henrick, K.; McPartlin, M. *J. Chem. Soc., Dalton Trans.* **1986**, 2259.
(28) Ge, Y.-W.; Sharp, P. R. *Organometallics* **1988**, *7*, 2234.
(29) Blake, A. J.; Cockran, R. W.; Ebsworth, E. A. V.; Holloway, J. H. *J. Chem. Soc., Chem. Commun.* **1988**, 529.
(30) Williams, G. L.; Whittle, R. R.; Geoffroy, G. L.; Rheingold, A. L. *J. Am. Chem. Soc.* **1987**, *109*, 3936.

Scheme VII

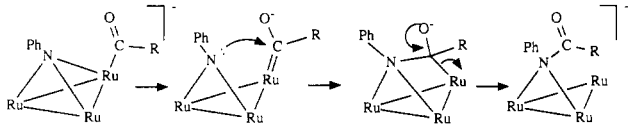

the latter through the important oxycarbene resonance form, the carbene–imido (eq 20) and acyl–imido (eq 16) coupling reactions are obviously similar, and a mechanism like that drawn in Scheme VII can be invoked for the latter. Indeed, carbene and carbonyl ligands are isolobal, and the observed acyl–imido, carbene–imido, and carbonyl–imido coupling reactions discussed herein are likely connected via a single mechanistic path as a comparison of the structures drawn in Schemes III and VII and eq 20 illustrates.

The reactions described herein effectively model several of the mechanistic steps illustrated in Scheme I for the proposed "imido" mechanism for the catalysis of nitroaromatic carbonylation. The most significant aspect of this work is the demonstration that halides promote both the formation of imido ligands from nitrosobenzene and their carbonylation to form isocyanates. The latter is particularly important since this reaction is difficult to achieve in the absence of halides. Importantly, the observed halide ordering $Cl^- > I^-$ for both reactions is exactly that found by Cenini and co-workers[3] in their studies of nitroaromatic carbonylation catalysis (eq 1), suggesting that the reactions reported herein may effectively model transformations that occur in this important catalytic process. However, it is clear that the entire mechanistic picture is far from being fully elucidated, and further studies are clearly necessary. Important to determine will be the process by which nitrobenzene initially enters the catalytic cycle. The results discussed above show that halides do not significantly effect the rate of formation of imido ligands from nitrobenzene, at least under our experimental conditions. It should be noted that recent studies by Belousov et al.,[5a] Gladfelter et al.,[5a] and unpublished work in our laboratories indicate that this substrate is activated by an electron-transfer path. It should also be recalled that there is no conclusive evidence that imido ligands or clusters are at all involved in the catalytic chemistry, and alternative mechanisms may operate. For example, isocyanates could form via β-hydride elimination from mononuclear carbamoyl complexes, as illustrated in eq 21.[6,31] Further studies aimed at elucidating the likelihood of these and related transformations are currently in progress.

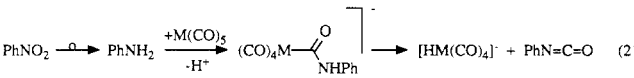

Experimental Section

General Data. The compounds $K[Co(CO)_4]$,[32] $Ru_3(CO)_{12}$,[33] $FeRu_2(CO)_{12}$,[34] $Fe_2Ru(CO)_{12}$,[34] $Ru_3(\mu_3\text{-NPh})_2(CO)_9$[10] $[PPN][Ru_3(CN)(CO)_{11}]$,[9b] and $[NEt_4][HRu_3(CO)_{11}]$[35] were synthesized by literature procedures, and the [PPN]X (X = Br, I, CN) salts were prepared from [PPN]Cl (Aldrich) by metathesis with the appropriate potassium salts. All solvents were dried by standard methods, and all manipulations were conducted under N_2 by using standard Schlenk techniques. Elemental analyses were performed by Schwartzkopf Microanalytical Laboratory, Woodside, NY.

Preparation of $[PPN][Ru_3(\mu_3\text{-NPh})(X)(CO)_9]$. Method A from $Ru_3(\mu_3\text{-NPh})(CO)_{10}$ (1). To a solution of 1 (50 mg, 0.078 mmol) in THF (30 mL) was added a slight excess of the appropriate [PPN]X salt followed by stirring for 2 h. After the initial bright yellow color had changed to dark orange, the solution was filtered through Celite and evaporated to dryness under vacuum. The residue was dissolved in CH_2Cl_2 (20 mL), and hexane was slowly added to precipitate the product which was isolated as a dark red solid. The yields were quantitative by IR, and isolated yields were 92% for Cl^- (**4a**), 96% for Br^- (**4b**), 94% for I^- (**4c**), and 89% for CN^- (**4d**). The $[Na(18\text{-crown-6})][Ru_3(\mu_3\text{-NPh})(I)(CO)_9]$ salt **4c'** was similarly prepared by the addition of NaI to 1 in the presence of 18-crown-6.

4a: IR (THF) ν_{CO} = 2070 (m), 2040 (s), 2016 (s), 1991 (s), 1962 (m), 1903 (w), 1705 cm^{-1}. Anal. Calcd for $C_{51}H_{35}O_9ClN_2P_2Ru_3 \cdot CH_2Cl_2$: C, 47.85; H, 2.84. Found: C, 47.82; H, 2.84.

4b: IR (THF) ν_{CO} = 2070 (m), 2041 (vs), 2018 (s), 1989 (s), 1941 (w, sh), 1907 (w), 1707 (w) cm^{-1}. Anal. Calcd for $C_{51}H_{35}O_9BrN_2P_2Ru_3$: C, 48.42; H, 2.77. Found: C, 48.49; H, 3.04.

4c: IR (THF) ν_{CO} = 2070 (m), 2039 (vs), 2016 (s), 1991 (s), 1705 (w) cm^{-1}. Anal. Calcd for $C_{51}H_{35}O_9IN_2P_2Ru_3$: C, 46.68; H, 2.67. Found: C, 46.15; H, 2.56.

4c': IR (THF) ν_{CO} = 2070 (m), 2039 (s), 2014 (s), 1991 (s), 1705 (w) cm^{-1}. Anal. Calcd for $C_{27}H_{29}O_{15}INNaRu_3$: C, 30.51; H, 2.73. Found: C, 30.13; H, 2.83.

4d: IR (THF) ν_{CO} = 2074 (m), 2047 (s), 2026 (s), 1995 (s), 1701 (w) cm^{-1}. Anal. Calcd for $C_{52}H_{35}O_9N_3P_2Ru_3$: C, 51.27; H, 2.89. Found: C, 51.07; H, 3.76.

Method B from $[Ru_3(X)(CO)_n]^-$ and Nitrosobenzene. To a solution of $Ru_3(CO)_{12}$ (50 mg, 0.078 mmol) in THF (40 mL) was added 1.1 equiv of the appropriate [PPN]X salt followed by stirring under N_2 for 2 h at 22 °C. The reaction mixture was then purged with N_2 for 40 min to form dark red solutions of $[PPN][Ru_3(\mu\text{-X})(CO)_{10}]$ (X = Cl, Br, I). For the preparation of $[PPN][Ru_3(CN)(CO)_{11}]$, the purging step was avoided to minimize the formation of $[PPN][Ru_6(CN)_2(CO)_{20}]$.[9b] Nitrosobenzene (12 mg, 0.11 mmol) was added to these solutions at room temperature while stirring. Complete reaction occurred over the course of 1 h to give burgundy-red solutions of **4a–d**. IR analysis indicated quantitative reaction in each case, although no attempts were made to isolate the products as crystalline solids since they were more conveniently prepared by method A above. The CO_2 product of the reaction between $[Ru_3(\mu\text{-Cl})(CO)_{10}]^-$ and PhNO was identified by IR analysis of the reaction mixture (ν_{CO} = 2338 cm^{-1}) and by high-resolution mass spectral analysis. For the latter, the CO_2 was isolated by bubbling N_2 through the reaction mixture and collecting the condensable gases in an LN_2 cooled trap. Calcd for CO_2: m/z = 43.9898. Found: m/z = 43.9866.

Preparation of $[HRu_3(\mu_3\text{-NPh})(CO)_9]^-$ (4e) from the Reaction of $[HRu_3(CO)_{11}]^-$ with PhNO. The salt $[NEt_4][HRu_3(CO)_{11}]$ (84 mg, 0.113 mmol) was dissolved in CH_2Cl_2 (30 mL), and PhNO (12 mg, 0.112 mmol) was added followed by stirring under N_2. IR analysis indicated complete conversion after 100 min. Evaporation of solvent and recrystallization gave the known compound **4e** as a red solid in 86% yield (76 mg, 0.097 mmol).

4e: IR (CH_2Cl_2) ν_{CO} = 2093 (w), 2054 (sh), 2025 (vs), 1992 (s), 1967 (s) cm^{-1}.

Preparation of $Ru_3(\mu_3\text{-NPh})(CO)_{10}$ by Reaction of $Ru_3(CO)_{11}(CH_3CN)$ with PhNO. $Ru_3(CO)_{12}$ (40 mg, 0.063 mmol) and CH_3CN (0.5 mL) were dissolved in THF (40 mL) followed by dropwise addition of Me_3NO (5 mg in 1 mL of MeOH) until the 2060 cm^{-1} IR band of $Ru_3(CO)_{12}$ disappeared. To the $Ru_3(CO)_{11}(CH_3CN)$ complex formed in this reaction was added PhNO (7 mg, 0.065 mmol) while stirring under N_2. IR analysis indicated complete reaction within 2 min. The solvent was removed by rotary evaporation, and the residue was chromatographed on silica gel using hexane as eluent. The first yellow band was $Ru_3(CO)_{12}$ (11 mg) which was followed by a yellow band of $Ru_3(\mu_3\text{-NPh})(CO)_{10}$ (22 mg, 72%).

Preparation of $Os_3(\mu_3\text{-NPh})(CO)_{10}$ by Reaction of

(31) See also: Dombeck, B. D.; Angelici, R. J. *J. Organomet. Chem.* **1977**, *134*, 203.
(32) Ellis, J. E.; Flom, E. A. *J. Organomet. Chem.* **1975**, *99*, 263.
(33) Eady, C. R.; Jackson, P. F.; Johnson, B. F. G.; Lewis, J.; Malatesta, M. C.; McPartlin, M.; Nelson, W. J. H. *J. Chem. Soc., Dalton Trans.* **1980**, 383.
(34) (a) Knight, J. A.; Mays, M. J. *J. Chem. Soc., Chem. Commun.* **1970**, 1006. (b) Yawney, D. B. W.; Stone, F. G. A. *J. Chem. Soc. A* **1969**, 502.
(35) (a) Johnson, B. F. G.; Lewis, J.; Raithby, P. R.; Suss-Fink, G. *J. Chem. Soc., Dalton Trans.* **1979**, 1356. (b) Keister, J. B. *J. Chem. Soc., Chem. Commun.* **1979**, 214.

$Os_3(CO)_{11}(CH_3CN)$ with PhNO. $Os_3(CO)_{12}$ (87 mg, 0.096 mmol) and CH_3CN (0.3 mL) were dissolved in THF (40 mL) followed by dropwise addition of Me_3NO (10 mg in 1 mL of MeOH) until the 2068 cm^{-1} IR band of $Os_3(CO)_{12}$ disappeared. To the $Os_3(CO)_{11}(CH_3CN)$ complex formed in this reaction was added PhNO (12 mg, 0.11 mmol) while stirring under N_2. IR analysis indicated complete reaction in 10 min, and workup as described above gave yellow $Os_3(\mu_3\text{-NPh})(CO)_{10}$ in 40% yield (33 mg; IR (hexane) ν_{CO} = 2074 (vs), 2026 (s), 2004 (m), 1694 (w) cm^{-1}).

Preparation of $Fe_2Ru(\mu_3\text{-NPh})(CO)_{10}$ (6). The cluster $Fe_2Ru(CO)_{12}$ (50 mg, 0.090 mmol) was dissolved in THF (30 mL) containing 3–4 drops of CH_3CN and cooled to 0 °C. A solution of Me_3NO (10 mg, 0.14 mmol) in MeOH (1 mL) was added carefully until the IR bands of $Fe_2Ru(CO)_{12}$ had just disappeared, indicating the formation of $Fe_2Ru(CO)_{11}(CH_3CN)$ {IR (THF) ν_{CO} = 2089 (w), 2029 (vs), 2008 (m, sh), 1807 (w, br) cm^{-1}}. To this cold reaction mixture was added PhNO (21 mg, 0.20 mmol), and the color immediately turned from light purple to yellow. After the solution was warmed to room temperature, the solvent was removed under vacuum, and the residue was chromatographed on silica gel using hexane as eluent. The first fraction to elute was a small yellow band of $Ru_3(CO)_{12}$ followed by a purple band of unreacted $Fe_2Ru(CO)_{12}$ (9 mg). The third band contained $Fe_2Ru(\mu_3\text{-NPh})(CO)_{10}$ (**6**) which was isolated as a yellow solid by solvent evaporation (15 mg, 34%). Some experiments using longer reaction times gave a small quantity (<5%) of $Fe_2Ru(\mu_3\text{-NPh})_2(CO)_9$ (**7**), which separated between the second and third chromatography fractions.

6: IR (hexane) ν_{CO} = 2099 (w), 2064 (vs), 2053 (vs), 2031 (s), 2022 (m), 1738 (w) cm^{-1}; MS (EI) m/z = 557 (M^+ – CO). Anal. Calcd for $C_{16}H_5O_{10}Fe_2NRu$: C, 32.89; H, 0.89. Found: C, 32.60; H, 0.96.

7: IR (hexane) ν_{CO} = 2095 (w), 2064 (vs), 2033 (s), 2012 (m), 1981 (w), 1953 (w) cm^{-1}; MS (EI): m/z = 620 (M^+ – CO).

Preparation of $FeRu_2(\mu_3\text{-NPh})(CO)_{10}$ (5). To a 0 °C solution of $FeRu_2(CO)_{12}$ (100 mg, 0.17 mmol) in THF (50 mL) containing 3–4 drops of CH_3CN were added Me_3NO and PhNO to form $FeRu_2(CO)_{11}(CH_3CN)$ {IR (THF) ν_{CO} = 2026 (vs), 1975 (sh), 1952 (w) cm^{-1}}. After the solution was warmed room temperature, the solvent was removed under vacuum and the residue was chromatographed on silica gel using hexane as eluent. The first fraction was a yellow band containing a trace of $Ru_3(CO)_{12}$ followed by a purple band of unreacted $FeRu_2(CO)_{12}$ (46 mg). The third band contained $FeRu_2(\mu_3\text{-NPh})(CO)_{10}$ (**5**), which was isolated as a yellow solid by solvent evaporation (20 mg, 35%).

5: MS (EI) m/z = 631 (M^+). IR (hexane) ν_{CO} = 2101 (w), 2072 (s), 2058 (vs), 2031 (s), 2024 (sh), 2012 (w), 1740 (w) cm^{-1}. Anal. Calcd for $C_{16}H_5O_{10}FeNRu_2$: C, 30.43; H, 0.79. Found: C, 30.69; H, 0.98.

Preparation of $Ru_3(\mu_3\text{-NPh})(\mu_3\text{-NR})(CO)_9$ (R = Ph, ^{t}Bu) by Reaction of $Ru_3(\mu_3\text{-NPh})(CH_3CN)(CO)_9$ with RNO. The cluster $Ru_3(\mu_3\text{-NPh})(CO)_{10}$ (**1**) (50 mg, 0.074 mmol) and CH_3CN (0.1 mL) were dissolved in CH_2Cl_2 followed by dropwise addition of Me_3NO (9 mg in 0.5 mL of MeOH) until the IR bands of **1** had been replaced by new bands at 2086 (w), 2054 (s), 2031 (vs), 2014 (m), and 1709 (w) cm^{-1} attributed to $Ru_3(\mu_3\text{-NPh})(CO)_9(CH_3CN)$. To this solution was added a slight excess of PhNO. After 10 min the solvent was removed by rotary evaporation. The residue was chromatographed on silica gel using hexane as eluent from which a single orange band eluted. Evaporation of solvent from this fraction left the known cluster $Ru_3(\mu_3\text{-NPh})_2(CO)_9$ (27 mg, 49%) as an orange microcrystalline solid. A similar reaction using Bu^tNO in place of PhNO gave $Ru_3(\mu_3\text{-NPh})(\mu_3\text{-NBu}^t)(CO)_9$ (**8**, 31 mg, 58%).

8: IR (CH_2Cl_2) ν_{CO} = 2099 (w), 2069 (m), 2043 (vs), 2024 (w), 2011 (w), 1991 (s) cm^{-1}; ^1H NMR ($CDCl_3$) δ 7.29–6.80 (br m, 5 H), 1.11 (s, 9 H); MS (EI) m/z = 689 (M^+ – CO).

Preparation of $[PPN][Ru_3(\mu_3\text{-NPh})_2(X)(CO)_8]$. To a THF (30 mL) solution of $Ru_3(\mu_3\text{-NPh})_2(CO)_9$ (40 mg, 0.054 mmol) was added a slight excess of [PPN]Cl, $[Et_4N]$Br, or [PPN]I. The solution was stirred for 6 h during which time the color change from orange to dark red. After the solution was filtered through Celite, the solvent was removed by evaporation under vacuum to leave a residue which was recrystallized from CH_2Cl_2/hexane. Isolated yields were 90% for Cl (**9a**), 88% for Br (**9b**), and 93% for I (**9c**).

9a: IR (THF) ν_{CO} = 2086 (m), 2011 (vs), 1975 (s), 1936 (m), 1910 (m), 1779 (w) cm^{-1}. Anal. Calcd for $C_{56}H_{40}ClO_8N_3P_2Ru_3$: C, 52.38; H, 3.12. Found: C, 52.10; H, 3.92.

9b: IR (THF) ν_{CO} = 2090 (w), 2012 (vs), 1990 (s), 1940 (m), 1926 (m, sh), 1987 (w) cm^{-1}. Anal. Calcd for $C_{28}H_{30}BrO_8N_3Ru_3$: C, 36.56; H, 3.26. Found: C, 36.03; H, 3.85.

9c: IR (THF) ν_{CO} = 2060 (m), 2020 (vs), 1998 (s), 1979 (m), 1950 (m) cm^{-1}. Anal. Calcd for $C_{56}H_{40}N_3O_8P_2IRu_3$: C, 48.76; H, 2.90. Found: C, 47.81; H, 3.42.

Carbonylation of the Clusters $[Ru_3(\mu_3\text{-NPh})(X)(CO)_9]^-$ (4a–e). THF solutions of the clusters **4a–e** were degassed by three freeze–pump–thaw cycles, and 1 atm of CO was introduced at 22 °C while stirring. Over the course of 30 min to 8 h the IR bands of the starting clusters **4a–c** were replaced by the bands of the clusters $[Ru_3(X)(CO)_{11}]^-$ (X = Cl, Br) or $[Ru_3(\mu_2\text{-I})(CO)_{10}]^-$ along with a band at 2260 cm^{-1} due to PhN=C=O. The latter product from the reaction of **4a** with CO was also characterized by the addition of MeOH to form methyl *N*-phenylcarbamate in 45% yield. The latter was isolated by chromatography on a silica TLC plate using 5/1 (v/v) hexane/CH_2Cl_2 as eluent. Clusters **4d** and **4e** failed to react with CO under these conditions. Half-lives for the carbonylation reactions were determined by monitoring the IR spectrum as the reaction progressed with the temperature maintained at 22 ± 0.2 °C with vigorous stirring.

Preparation of $HCoRu_2(\mu_3\text{-NPh})(CO)_9$ (11). The cluster $Ru_3(CO)_{12}$ (0.10 g, 0.15 mmol) and $K[Co(CO)_4]$ (0.032 g, 0.15 mmol) were combined in a 25-mL two-neck flask equipped with an N_2 inlet and a reflux condenser, and THF (20 mL) was added. The yellow mixture was refluxed for 1 h and then cooled to 22 °C to give a gold-colored solution showing IR bands at 2069 (w), 2002 (s), and 1963 (vs) cm^{-1} due to the anion $[CoRu_2(\mu_3\text{-NPh})(CO)_9]^-$. This solution was then cooled to −78 °C, and $HBF_4\cdot Et_2O$ was added dropwise via syringe until IR monitoring indicated complete reaction. After the yellow solution was stirred for 1 h while being warmed to 22 °C, the solvent was removed by evaporation to leave a yellow solid which was dissolved in hexane and chromatographed on silica gel using hexane as eluent. This gave one yellow band of **11** which was isolated as a yellow microcrystalline solid by solvent evaporation (85 mg, 0.14 mmol, 85%).

11: IR (hexane) ν_{CO} = 2102 (vw), 2077 (s), 2046 (vs), 2029 (vs), 2013 (w) cm^{-1}; MS (FD) m/z = 606 (M^+ – CO); ^1H NMR (acetone-d_6, 25 °C) δ 7.3–7.0 (m, Ph), −15.65 (s, M–*H*). Anal. Calcd for $C_{15}H_6CoNO_9Ru_2$: C, 27.67; H, 1.10. Found: C, 27.82; H, 1.15.

Preparation of $[PPN][CoRu_2(\mu_3\text{-NPh})(CO)_9]$ (10). To a THF (50 mL) solution of cluster **11** (20 mg, 0.033 mmol) was added [PPN]Cl (20 mg, 0.035 mmol). The color of the solution immediately changed from yellow to dark orange as cluster **10** formed. This species was isolated as an air-stable microcrystalline solid by solvent evaporation and recrystallization from pentane (30 mg, 0.026 mmol, 80% yield).

10: IR (THF) ν_{CO} = 2999 (s), 1965 (vs), 1959 (m) cm^{-1}; ^1H NMR (22 °C, acetone-d_6) δ 7.70–6.90 (m, Ph). Anal. Calcd for $C_{51}H_{35}CoN_2O_9P_2Ru_2$: C, 53.60; H, 3.06. Found: C, 52.99; H, 2.78.

Carbonylation of $[PPN][CoRu_2(\mu_3\text{-NPh})(CO)_9]$ (10). This salt was dissolved in THF (25 mL) and placed in a Fischer-Porter bottle under 70 psi of CO. The solution was heated to 100 °C for 8 h and then cooled to room temperature and vented. IR analysis of the resulting yellow solution showed that complete reaction had occurred to form $Ru_3(CO)_{12}$ {2060 (s), 2031 (s), 2012 (vs) cm^{-1}}, $[Co(CO)_4]^-$ {1886 (s) cm^{-1}}, and $[PhNCO]_2$ {1778 (s) cm^{-1}}. No reaction occurred when milder carbonylation conditions were employed (22 °C, 1 atm of CO, 4 h).

Preparation of $[Ru_3(\mu_3\text{-NPh})(CO)_9(C\{O\}R)]^-$. The cluster $Ru_3(\mu_3\text{-NPh})(CO)_{10}$ (**1**), (50 mg, 0.074 mmol) was dissolved in Et_2O (40 mL), and the solution was cooled to −78 °C by using a dry ice/acetone bath. To this solution was added dropwise a hexane solution of MeLi or PhLi until the major IR bands of **1** disappeared. During this time, a yellow precipitate of $[Ru_3(\mu_3\text{-NPh})(CO)_9(C\{O\}R)]^-$ (**14**, R = Me; **15**, R = Ph) deposited. The solvent was decanted slowly, and the precipitate was washed with hexane until the extracts were colorless. IR analysis of the residue showed it to consist of mainly **14** (or **15**) contaminated with a small amount of **16** (or **17**). The facile conversion of **14** into **16** and **15** into **17** precluded the isolation of a pure sample of either compound.

14: IR (THF) ν_{CO} = 2066 (m), 2033 (s), 2010 (vs), 1993 (m), 1971 (s), 1946 (m), 1685 (w), 1587 (w) cm^{-1}.

15: IR (THF) ν_{CO} = 2066 (w), 2045 (m), 2012 (s), 1973 (vs), 1954 (m), 1931 (m, sh), 1680 (w), 1536 (w) cm^{-1}.

Carbonylation of $[Ru_3(\mu_3\text{-NPh})(CO)_9(C\{O\}R)]^-$ To Form $[Ru_3(\mu_2\text{-N(Ph)C\{O\}R})(CO)_{10}]^-$. Clusters **14** and **15** were prepared from complex **1** (70 mg, 0.10 mmol) as described above and redissolved in THF (40 mL). The solutions were placed under 1 atm of CO after degassing by three freeze–pump–thaw cycles. The color changed from red to orange over the course of 1 h as the amido clusters $[Ru_3(\mu_2\text{-N(Ph)C\{O\}R})(CO)_{10}]^-$ (**16**, R = Me; **17**, R = Ph) formed. Tetramethylethylenediamine (TMEDA, 0.3 mL) was added to the reaction mixture and the solvent was evaporated under vacuum. All attempts to recrystallize the resultant residue left the $[Li(TMEDA)]^+$ salts of **16** and **17** as dark red oily solids. Yields of **16** and **17** were 65% and 54%, respectively.

16: IR (THF) ν_{CO} = 2070 (w), 2010 (s), 1985 (vs), 1954 (m), 1934 (m), 1809 (m), 1798 (m), 1530 (w) cm^{-1}; ^1H NMR ($CDCl_3$) δ 6.8–7.6 (br, Ph, 5 H), 1.56 (s, CH_3, 3 H); ^{13}C NMR ($CDCl_3$) δ 193.9, 192.3 (Ru–CO), 181.0 (C{O}Me), 154.6, 134.5, 130.4, 129.0 (NPh), 22.4 (CH_3). Anal. Calcd for $C_{24}H_{24}LiN_3O_{11}Ru_3{\cdot}2CH_2Cl_2$: C, 30.79; H, 2.76. Found: C, 30.10: H, 2.82.

17: IR (THF) ν_{CO} = 2062 (w), 2014 (s), 1987 (vs), 1964 (sh), 1809 (m), 1796 (m), 1541 (vw) cm^{-1}; ^{13}C NMR ($CDCl_3$) δ 193.9, 192.3 (Ru–*CO*), 186.3 (*C*{O}Ph), 147.3, 140.9, 137.4, 132.6, 132.3, 129.8 (Ph). Anal. Calcd for $C_{28}H_{26}LiN_3O_{10}Ru_3{\cdot}CH_2Cl_2$: C, 36.32; H, 2.92. Found: C, 35.5.: H, 3.39.

Protonation of $[Ru_3(\mu_2\text{-N(Ph)C\{O\}R})(CO)_{10}]^-$ To Form $HRu_3(\mu_2\text{-N(Ph)C\{O\}R})(CO)_{10}$. Clusters **16** and **17** were prepared in situ from complex **1** (50 mg, 0.074 mmol) and the appropriate RLi reagent in THF (40 mL), as described above. To these solutions was added excess HBF_4 at −78 °C, and the reactions were monitored by IR until the bands of **16** and **17** disappeared. The solutions were warmed to room temperature, the solvent was removed under vacuum, and the residue was chromatographed on silica gel using hexane as eluent. For **18** (R = Me) the first fraction to elute was a small yellow band of $Ru_3(CO)_{12}$ (5 mg) followed by a yellow band of **18** (16 mg, 32% from complex **1**). The third band contained colorless PhNHC{O}Me (2 mg, 20%) which was isolated as a white solid by solvent evaporation. For **19** (R = Ph), the first fraction was a yellow band of $Ru_3(CO)_{12}$ (8 mg) followed by a yellow band containing a trace of $H_2Ru_4(CO)_{13}$ and then a yellow band of **19** (12 mg, 21% from complex **1**). Traces of PhNHC{O}Ph were occasionally isolated after the yellow band of **19**.

18: IR (hexane) ν_{CO} = 2114 (w), 2105 (w), 2070 (s), 2056 (s), 2041 (m), 2026 (s), 2016 (vs), 1993 (m), 1944 (w), 1543 (w) cm^{-1}; ^1H NMR (acetone-d_6) δ 6.8–7.5 (br, Ph, 5 H), 1.56 (s, CH_3, 3 H), −15.02 (s, Ru–*H*, 1 H); MS (FAB) m/z = 662 (M^+ − 2CO).

19: IR (hexane) ν_{CO} = 2114 (w), 2103 (w), 2075 (sh), 2065 (s), 2054 (vs), 2028 (m), 2019 (s), 2011 (m), 2003 (m), 1550 (w) cm^{-1}; ^1H NMR (acetone-d_6) δ 6.8–7.8 (br, Ph, 12 H), −14.06 (s, Ru–*H*, 1 H; MS (FAB) m/z = 784 (M^+).

Carbonylation of 18 To Form PhNHC{O}Me. Complex **18** (30 mg, 0.042 mmol) was dissolved in THF (40 mL), and the solution was degassed by three freeze–pump–thaw cycles. The solution was then placed under 1 atm of CO at room temperature and left for 1 day. The solvent was evaporated, and the residue was chromatographed on a silica TLC plate using hexane as eluent. The first fraction to elude was a yellow band of $Ru_3(CO)_{12}$ (18 mg, 67%) followed by a colorless band of PhNHC{O}Me (3 mg, 53%) which was characterized by IR (ν_{CO} = 1696 cm^{-1}) and mass spectral analysis (m/z = 135 (M^+)).

Crystal Structure Determinations. Crystallographic data for **4c′** and **11** are summarized in Table I. For both structures, photographic evidence revealed no symmetry higher than triclinic, and the centrosymmetric alternative space group $P\bar{1}$ was initially suggested for both structures by the *E* statistics and confirmed by the chemically sensible results of refinement. The data for both were empirically corrected for absorption (Ψ-scans, 216 reflections, 10° steps). For **4c′**, T_{max}/T_{min} = 1.32, and for **11**, T_{max}/T_{min} = 1.27. Both structures were solved by direct methods and completed by difference Fourier techniques. All comparisons used SHELXTL (5.1) software (G. Sheldrick, Nicolet XRD, Madison, WI). Suitable crystals of **11** were obtained from a hexane solution by slow evaporation of solvent. Red crystals of **4c′** were obtained by slow diffusion of hexane into CH_2Cl_2 solutions of the compound. For **4c′**, some conformational ambiguity exists in the 18-crown-6 molecule although the usual (syn–anti–anti)$_6$ conformation prevails. All non-hydrogen atoms were anisotropically refined, and all hydrogen atoms were treated as idealized, updated isotropic contributions (d_{CH} = 0.96 Å).

The asymmetric unit of **11** contains two independent molecules, only one (designated by primed labels) of which is completely ordered. In the other molecule, Ru(2) and Co are disordered such that each site is approximately one-third the character of the other. The disordered metal atom occupancies of the composite atoms were refined after fixing the thermal parameters at the average (0.045 $Å^2$) for the metal atoms of the ordered molecule. From difference maps, the major and minor CO group environments were also located and refined at occupancies equal to the metal atom occupancies. The disordered molecule also contains a low occupancy (~20%) μ_3-CO labeled C(17) and O(17) located on the opposite side of the metal plane from the NPh group [Ru(1)–C(17), 2.33 (3) Å; Ru(2)–C(17), 2.26 (3) Å; Co–C(17), 2.14 (4) Å]. No adjustment of the occupancies of the other CO groups was made. With the exception of the mirror occupancy CO group atoms which were isotropically refined, all non-hydrogen atoms were refined with anisotropic thermal parameters. The μ-H atom in the ordered molecule was located and isotropically refined. The remaining hydrogen atoms were included as idealized (d_{CH} = 0.96 Å) and updated isotropic contributions (the μ-H atom of the disordered molecule was ignored). The phenyl rings were constrained to rigid, planar hexagons to conserve data (d_{CC} = 1.395 Å).

Complete tables of bond distances, angles, hydrogen atom positions, thermal parameters, and structure factors for **4c′** were deposited as supplementary material to ref 7. The corresponding data for **11** is included in the supplementary material for this paper.

Acknowledgment. We thank the Department of Energy, Office of Basic Energy Sciences, and the ARCO Chemical Co. for support of this research, the Johnson Matthey Co. for the generous loan of Ru salts, The National Science Foundation for partially funding the diffractometer at the University of Delaware, and R. Minard, J. Blank, G. Steinmetz, and R. Hale for recording mass spectra.

Registry No. **1**, 51185-99-0; **3a**, 117308-22-2; **3b**, 117308-23-3; **3c**, 117308-24-4; **3d**, 112785-95-2; **4a**, 110509-52-9; **4b**, 110509-54-1; **4c**, 110509-56-3; **4c′**, 110657-86-8; **4d**, 121471-52-1; **4e**[NEt_4], 121471-53-2; **5**, 121471-54-3; **6**, 121471-55-4; **7**, 121471-56-5; **8**, 121496-80-8; **9a**, 121471-58-7; **9b**, 121524-31-0; **9c**, 121471-60-1; **10**, 121471-63-4; **11**, 121471-61-2; **13**, 1025-36-1; **14**(Li), 121496-81-9; **15**(Li), 121471-64-5; **16**[Li(TMEDA)], 121471-66-7; **17**[Li(TMEDA)], 121471-68-9; **18**, 121471-69-0; **19**, 121471-70-3; $Ru_3(\mu_3\text{-NPh})_2(CO)_9$, 115826-82-9; $Ru_3(CO)_{12}$, 15243-33-1; $[NEt_4][HRu_3(CO)_{11}]$, 12693-45-7; PhNO, 586-96-9; $Ru_3(CO)_{11}(CH_3CN)$, 84896-12-8; $Os_3(\mu_3\text{-NPh})(CO)_{10}$, 102869-57-8; $Os_3(CO)_{11}(CH_3CN)$, 65702-94-5; $Os_3(CO)_{12}$, 15696-40-9; $Fe_2Ru(CO)_{12}$, 20468-34-2; $FeRu_2(CO)_{12}$, 12388-68-0; $Ru_3(\mu_3\text{-NPh})(CO)_9(CH_3CN)$, 121471-71-4; Bu^tNO, 917-95-3; $[Ru_3(\mu_2\text{-I})(CO)_{10}]$, 121471-72-5; PhN=C=O, 103-71-9; $K[Co(CO)_4]$, 14878-26-3; $[CoRu_2(\mu_3\text{-NPh})(CO)_9]^-$, 121471-62-3; CO, 630-08-0; MeLi, 917-54-4; PhLi, 591-51-5; PhNHC{O}Me, 103-84-4; PhN, 2655-25-6; MeOH, 67-56-1; PhCO, 2652-65-5; Bu^tCO, 50694-27-4; Ru, 7440-18-8; Fe, 7439-89-6; Co, 7440-48-4; methyl *N*-phenylcarbamate, 2603-10-3.

Supplementary Material Available: Tables of bond distances and angles, anisotropic thermal parameters, and hydrogen atom coordinates for **11** (6 pages); a listing of observed and calculated structure factors for **11** (31 pages). Ordering information is given on any current masthead page.